

AD-A237 646



2

Office of Naval Research Grant N00014-91-J-1317

"Bioacoustic Signal Classification in Cat Auditory Cortex"

DTIC
ELECTE
JUN 19 1991
S D D

1st Semiannual Progress Report
December 15, 1990 to June 14, 1991

Submitted by:

Dr. Christoph Schreiner
Dr. Mitchell Sutter
Diane Keeling
Dr. Kamil Grajski

DISTRIBUTION STATEMENT A
Approved for public release;
Distribution Unlimited

From:

Coleman Memorial Laboratory
W.M. Keck Center for Integrative Neuroscience
Department of Otolaryngology
School of Medicine
University of California, San Francisco
San Francisco, CA 94143-0732

91-02424



91 6 18 013

1. Cortical Physiology

Two of the main objectives of the grant are a) to determine which functionally significant acoustical parameters and/or physiological response parameters show a systematic spatial organization, as obtained with multiple unit mapping techniques, within the boundaries of the primary auditory cortex (AI) of the cat, and b) what single neuron response characteristics are underlying the systematic spatial signal representations as obtained with multiple unit measures. Knowledge of these parametric signal representations shall enable us to develop a basic understanding of cortical processing and its implications for the coding/classification of complex signals. Initially, cortical receptive fields for simple signal parameters, such as frequency, bandwidth, and intensity, will be explored before turning to more complex signal properties such as spectral shape or temporal variations. The following three subsections, describe some results or preliminary results regarding the frequency coding and the intensity coding of tones bursts, and the coding of broad-band spectra with complex spectral envelopes (ripple spectra).

Two other cortical recording projects are currently underway exploring the temporal response characteristics along the isofrequency domain in AI, and the bandwidth organization in the anterior auditory field. Although it is too early to report in detail our findings, preliminary analysis indicated that there is a systematic change in the latency of the response onset along the isofrequency domain. In addition, many cortical locations show a second response that occurs 50 to 250 ms after the initial onset response. This response does not represent an offset response since it is also present when the stimulus duration is extended to more than 500 ms. The timing of the second response appears to be largely independent from the onset response. The data suggest a systematic variation of the latency of the second response along the isofrequency domain of AI. Preliminary data from the mapping of the anterior auditory field indicate that an organization of the integrated excitatory bandwidth exists that is quite similar to that seen in AI. It appears that the width of the sharply tuned area may be narrower than that in AI.

1.1 Sharpness of frequency tuning in AI

The summary and main conclusions of this portion of the studies are outlined below. A description of the used methods, detailed results and a discussion of the findings are attached as Appendix B in the form of a manuscript submitted for publication in the Journal of Neurophysiology.

The spatial distribution of the sharpness of tuning of single neurons along the isofrequency domain of primary auditory cortex (AI) was studied. The sharpness of tuning gradient was obtained with multiple unit recordings, and in combination with the cochleotopic organization, served as a frame of reference for the locations of single neurons. The frequency selectivity or 'integrated excitatory bandwidth' of multiple units varied systematically along isofrequency contours in AI (see Figs. 2 to 4, Appendix A). The most sharply tuned unit clusters were found at the approximate center of essentially dorso-ventrally oriented isofrequency contours. A gradual broadening of the integrated excitatory bandwidth in both dorsal and ventral directions was

consistently seen.

The multiple unit measures of the bandwidth 10 dB (BW10) and 40 dB (BW40) above minimum threshold, pooled across several animals and expressed in octaves, were similar to those described within individual cases in cats. As in the individual animals, the bandwidth maps were V-shaped with minima located at the approximate center of the dorsal-ventral extent of isofrequency contours in AI. The location of the minimum in the multiple unit bandwidth map (i.e. the most sharply tuned area) was used as a reference point to pool single neuron data across animals.

For single neurons, the dorsal half of the BW40 distribution showed a gradient paralleling that of multiple units (Fig. 5, Appx. A). For both single and multiple units, the average excitatory bandwidth increased at a rate of approximately 0.27 octaves per millimeter from the center of AI toward the dorsal fringe. Differing from the dorsal half of AI, the ventral half of AI showed no clear BW40 gradient for single units along its dorso-ventral extent. At 40 dB above minimum threshold, most ventral neurons encountered were sharply tuned. By contrast, the multiple unit BW40 showed a gradient similar to the dorsal half with 0.23 octaves per millimeter increasing from the center toward the ventral border of AI.

For single neurons, BW10 showed no clear systematic spatial distribution in AI. Neither the dorsal nor the ventral gradient was significantly different from zero slope although the dorsal half showed a trend toward increasing BW10s (Fig. 7, Appx. A). Contrasting single neurons, both dorsal and ventral halves of AI showed BW10 slopes for multiple units confirming a V-shaped map of the integrated excitatory bandwidth within the isofrequency domain.

Based on the distribution of the integrated (multiple unit) excitatory bandwidth, AI was parceled into three regions: the dorsal gradient, the ventral gradient, and the central narrowly tuned area. In ventral AI, single units were significantly more sharply tuned than multiple units for BW10 and BW40. In dorsal AI, single units were not statistically different from multiple units for BW40. In central AI, single units were significantly sharper for BW40, but not BW10 (Fig. 6 and 8, Appx. A).

Estimates of the scatter of best frequency (BF) of single neurons in the isofrequency domain were obtained relative to the fairly smooth frequency organization as determined with multiple units. The central narrowly tuned region showed the least BF scatter (Fig. 9 of Appx. A). The BF scatter increased toward the dorsal, and in particular, the ventral end of the isofrequency domain.

The combined single and multiple unit results suggest that AI is composed of at least two functionally distinct sub-regions along the isofrequency domain based on the bandwidth properties of tuning curves. The dorsal region (AId) displays a gradient of BW40 expressed in single and multiple unit measurements, and contains broadly and sharply tuned single-peaked as well as multi-peaked neurons. The ventral region (AIv) predominantly contains neurons narrowly tuned at 40 dB above threshold. The increase in integrated (multiple-unit) excitatory bandwidth in AIv can be related to a progressively larger BF scatter at more ventral locations. The transition

between AI_d and AI_v is delineated by a reversal in the BW40 gradient for multiple units coinciding with a region of small BF scatter of the underlying single neurons.

1.2. Response threshold distribution in AI

Previous mapping studies in this laboratory indicated that the response thresholds of groups of neurons showed a systematic distribution along the isofrequency domain of AI (Schreiner, Mendelson, and Sutter (manuscript in preparation)). Fig. 1 illustrates an example of the distribution of minimum thresholds (i.e. threshold at CF) for multiple unit recordings in AI. Note the minimum along the dorso-ventral (isofrequency) extent of AI. The minimum is situated at the approximate location of neuron clusters that exhibit the narrowest excitatory bandwidth (see above). Similar alignments of locations with highest sensitivity and narrowest frequency tuning were seen in other studied cases.

Evaluation of the monotonicity of rate-level functions of multiple unit responses also revealed a strong tendency for a systematic spatial arrangement. Cortical locations with highly non-monotonic rate-level functions were clustered in two regions of AI. One region coincided with the area of sharpest frequency tuning (smallest integrated excitatory bandwidth) as well as lowest response thresholds within the isofrequency domain. A second area of high non-monotonicity was usually located approximately 3 mm more dorsally (see example in Figure 2).

Preliminary analysis of the response threshold and monotonicity of 108 topographically localized single revealed the following points (Sutter and Schreiner, manuscript in preparation):

In ventral AI, the spatial distribution of single neuron monotonicity paralleled the shape of multiple unit monotonicity. In dorsal AI, the monotonicity of pooled single neurons did not display any clear topography directly related to the multiple unit topography of monotonicity.

The response threshold of neurons along the isofrequency domain showed a characteristic distribution. The threshold range for single neurons displayed two minima along the isofrequency domain. These two locations were aligned with the two regions that showed high non-monotonicity of rate-level functions in the multiple unit recordings. Regions not showing high non-monotonicity of their rate-level functions showed a substantially larger scatter in response thresholds (see Fig.3 upper panel). The region coinciding with the sharpest frequency tuning exhibited the lowest average threshold, the smallest threshold scatter (see Fig. 3 lower panel) and a high degree of non-monotonicity.

The spatial alignment of a) narrow frequency tuning, b) narrow amplitude tuning (reflected in strongly non-monotonic rate-level functions), and c) narrow range of low thresholds in the approximate dorso-ventral center of AI suggests a special functional role for this about one mm wide strip across all frequencies. A possible interpretation of this constellation is that of a low intensity signal detector or 'fovea' which analyses with great spectral resolution signals that are just above the background noise. This interpretation is supported by findings of other

investigators that have shown that non-monotonic rate-level functions are shifted to higher levels when tones are presented in the presence of continuous background noise. In other words, the receptive field of the 'foveal' neurons is always tuned to those sound intensities that are just above the background noise. According to plan, this hypothesis will be tested in the second and third year of funding.

Preliminary results from recent mapping experiments in the auditory cortex of owl monkeys (Merzenich et al. 1991, see reference list in Appendix A) suggest that similar organizations are present in this primate, and therefore, indicate that the described spatial organizations in cat auditory cortex may indeed reflect general mammalian processing strategies.

1.3 Complex spectral shape

The demonstration of a ventral and a dorsal gradient in integrated excitatory bandwidth along the isofrequency domain of AI, in combination with the dorso-ventral differences in single unit tuning, suggests that cortical neurons with the same CF may respond differently to broad band stimuli. That this is indeed the case for click-like stimuli has been demonstrated by us in a recent publication (Schreiner and Mendelson 1990 (see reference list in Appendix A)). The finding of a range of excitatory bandwidths, either due to broadening of the receptive field of single neurons or reflecting an increase of the CF variance of sharply tuned neurons at a given location, also suggest a selectivity of neurons for certain broad band stimuli that have spectral envelopes features closely corresponding to the cells receptive field.

The use of a signal with parametrically well controllable spectral envelopes would be instrumental in studying those phenomena. Fig. 4 shows the spectra of three broad band stimuli with a regular modulation of the spectral envelope that will be employed in our studies. The signal has a harmonic structure (e.g. a fundamental frequency of 100 Hz) and a sinusoidally modulated spectral envelope (on a logarithmic frequency scale). The tilt of the harmonic spectrum assures that the signal has equal energy per octave. Three spectral modulation frequencies -- or ripple densities measured in ripples per octave -- are demonstrated. In general, this type of signal corresponds to sinusoidal luminance gratings widely applied in visual research. However, the significance of this type of signal continuum for auditory neurophysiology is much higher since ripple spectra are a generalized representation of an important aspects of animal communication, namely that of resonances in the vocal tract. In addition, modulations in the spectral envelope of broad band stimuli are a common characteristic of environmental sounds.

The three most important signal parameters of ripple spectra are the ripple density (or spectral modulation frequency), the ripple phase (phase of spectral modulation frequency or frequency position of ripples) and the ripple depth (modulation depth of spectral envelope). In Fig. 5, the response of a single neurons in AI of the cat to variations in the ripple density (fixed ripple phase, fixed ripple depth) and the ripple phase (fixed ripple density, fixed ripple depth) are illustrated. The upper panel shows that the response magnitude of the cell varied strongly with the ripple phase of the stimulus. Near the phase zero, i.e. a ripple maximum is located at the CF of

the neuron, the response is biggest and declines with shifts in the position of the ripples. The width and symmetry of this phase plot reflects characteristics of the receptive field of the neuron, including excitatory bandwidth and the effects of lateral inhibition. Since the stimulus is a broad band signal, the information about the response selectivity considerably expands our view of neurons as determined with narrow band (pure tone) stimuli. The lower panel of Fig. 5 shows an example of a ripple transfer function, that is the spacing/bandwidth of the ripples is changed systematically by keeping one of the ripples always centered at the CF of the neuron. Note that the cell was selective for ripple densities around 1.4 and did not respond well for ripple densities above 2 and below 0.5. (For the range of ripple densities in human vowels see below.) The response latency showed only minor effects with changes of the ripple density.

2. Behavioral Studies

Preparations for the setup to record from awake animals in a behavioral setting were initiated with the help of Dr. William Jenkins, our consultant for the behavioral methods and their implementation. A wire mesh cage, approximately 16" wide X 22" long X 18" high was built that will be used for animal psychophysical testing/ chronic cortical recording. For the behavioral rewards, a 6-oz metal syringe will dispense food paste via a pump, driven by a stepping motor. The syringe is connected by plastic tubing to a lick plate that has a small hole through which the paste is dispensed.

The animal will be trained to initiate a trial or recording period by pressing with its nose the center of three response keys. This will keep the head of the cat in a reproducible position allowing a calibration of the sound delivery. While the animal is holding the response key, a number of stimuli will be presented in free field and the cortical response will be recorded from chronic electrodes implanted into the cortex.

Currently, the stimulus delivery software is under development using the Labview development system on Apple II computers. A first version is operational that can deliver three stimuli after initialization by the animal. The program is currently tested in a human psychophysical task that is related to the perception of ripple spectra. Only little psychoacoustical data are available with regard to the perception and discrimination of ripple spectra. In order to understand the perceptual implications in using this stimulus continuum, we started a small series of psychophysical experiments that test those signal parameters that will be used in the animal experiments. This will allow us to estimate the behaviorally most relevant parameter range. From considerations of the nature of vowels, we can deduce the main range of ripple densities that are important for humans. Fig.6 shows the average first two formant frequencies of some English vowels for different speakers. In addition, the ripple densities for these formants are shown. From this graph and similar evaluations of the 2. and 3. formant, a range of ripple densities between 0.3 and 6 ripple/octave appears to be relevant. Note that the speaker dependent variability in the formant frequencies is considerably reduced in using the ripple description.

No data are available regarding the discrimination of ripple spectra subjected to shifts in

ripple phase (shift in formant frequencies). Figure 7 shows an example of the results in a human psychophysical test of the discrimination of relative ripple position. The phase of the spectral modulation frequency, i.e. the ripple phase is varied and the stimulus is compared to a stimulus with ripple phase zero. After completion of the human psychophysics, cats will be trained to perform the same test in order to compare their performance with humans. So far, the range of best ripple densities as obtained from cat cortical neurons is well within the range of the human estimates.

3. Computational Studies

3.1 Establishing an objective basis for evaluation of progress.

In addition to generating an understanding of the physiological mechanisms, one of the goals of the present study is to define and apply novel, 'biologically pre-processed' methods of representing complex acoustic waveforms for the purposes of signal recognition/classification. To that end, we will use recognition performance on the TI Digits Database as one benchmark with which to measure our progress. Our recognition system is based on hidden markov models encapsulated in the SPHINX recognition system developed by Kai-Fu Lee (now at Apple) and his colleagues. In a just-initiated project, we are cooperating with Malcolm Slaney and Dick Lyon at Apple Computers to use their cochlear model as a front-end. We are comparing performance with this novel front-end to the standard cepstral representation. Of course, this is only one of many potential alternative peripheral models/front ends we could use. We are in the process of establishing the use of other distributed front-end systems, namely that of our co-investigator Ted Lewis which includes properties of auditory nerve fibers in addition to cochlear processes.

As of this writing, we are obtaining a 4.62% error rate on the TI Digits test set using the standard SPHINX front-end (see below). (This is well short of the world's best mark of 1.4% achieved at AT&T by Rabiner and colleagues; however, our system is under continuous improvement with this goal in mind). Also as of this writing, we have preprocessed the TI Digits Database using the Lyon cochlear model and are evaluating training and recognition to iron out any changes required in the SPHINX system.

The (Adult) TI Digits Database consists of 225 speakers (M 111; F 114). The speaker set is dialectically balanced based on a partition of the US into 21 dialectical regions. The recorded utterances are digit sequences. The digits were "zero", "oh", "one", etc. Each speaker recorded 77 utterances: a.) 22 isolated digits; and b.) 11 each of two-, three-, four-, five- and seven-digit strings. Digit sequences were chosen at random. Recording conditions were controlled and the data is of high quality. (We have plenty of non-controlled recordings available for later testing.) The database is split into independent training (112 speakers) and testing subsets (113 speakers). The training set contains 8623 utterances and the testing set contains 8700 utterances. Other databases we may consider include the DARPA Resource Management Database (a standard dataset used by DARPA to evaluate contractors' performance) and several Apple in-house

speaker-dependent and speaker-independent databases.

The SPHINX system is a hidden markov model based training and recognition system. Training of hidden markov models is based on standard technology (Baum-Welch equations). Recognition is based on the standard beam search approach to pruning the search space. In the present system, data is initially represented in the form of a cepstrum. (To obtain a cepstrum, first generate an LPC-spectrum for each 10-20msec of speech, do a log transform of that spectrum and then inverse FFT it.) Sphinx uses the first 13 components of the cepstrum and vector quantizes that and several other cepstral-derived features. These other features include estimates of derivatives, energy, etc. In short, the SPHINX front-end codes each frame of speech as a symbol from each of several vector quantization codebooks. There is a real-time version of SPHINX running on a Mac.

The Lyon cochlear front-end is modified essentially to force a fit with the existing SPHINX system. The cochlear model represents input as firing probabilities. By a nonlinear adaptive gain control and filtering a cochleogram is produced. This cochleogram has the appearance similar to that of a spectrum.

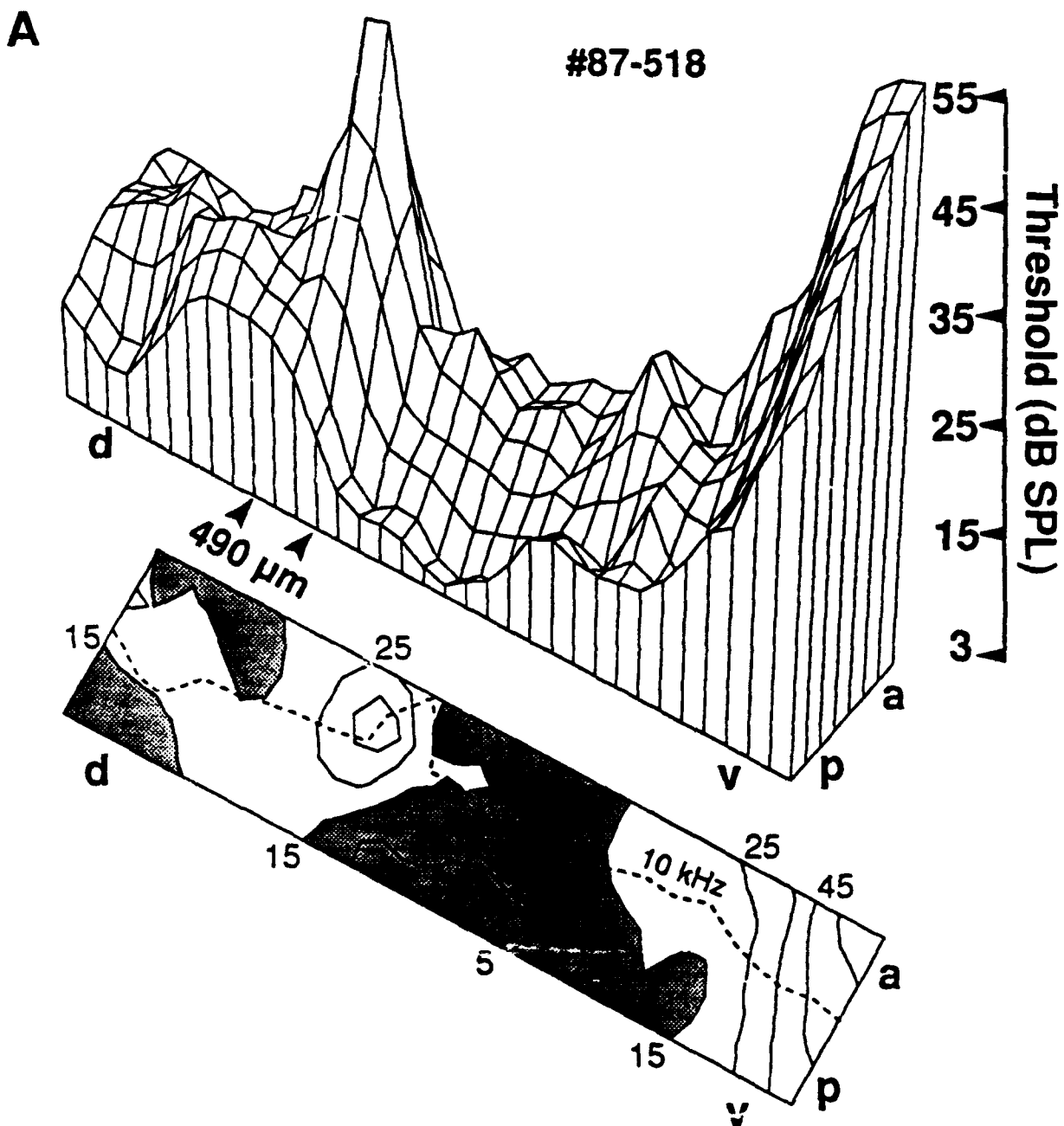


Figure 1: Spatial distribution of the contralateral response threshold in AI expressed in dB SPL. The upper portion depicts a pseudo three-dimensional projection of the spatial distribution of response thresholds in AI (case #87-518). Two dimensions of the projection represent the dorso-ventral (d,v) and posterior-anterior (p,a) extent of the cortical surface. The third dimension, elevation of the surface, corresponds to the magnitude of the functional parameter 'threshold' across the mapped cortex. An additional smoothing factor of 0.9 was applied to the data. Due to perspective distortion in the projection, the scale bar of the threshold axis is only accurate for the nearest corner of the plot. The lower portion of the panel shows an undistorted contour-plot representation of the same data. Each line connects points of equal threshold. Number next to some lines reflect the appropriate values of iso-threshold contours. Contour intervals correspond to 10 dB steps. Shaded areas correspond to locations with threshold values below 15 dB SPL. The orientation of the isofrequency domain of the mapped cortex is indicated by the dashed line (10 kHz).

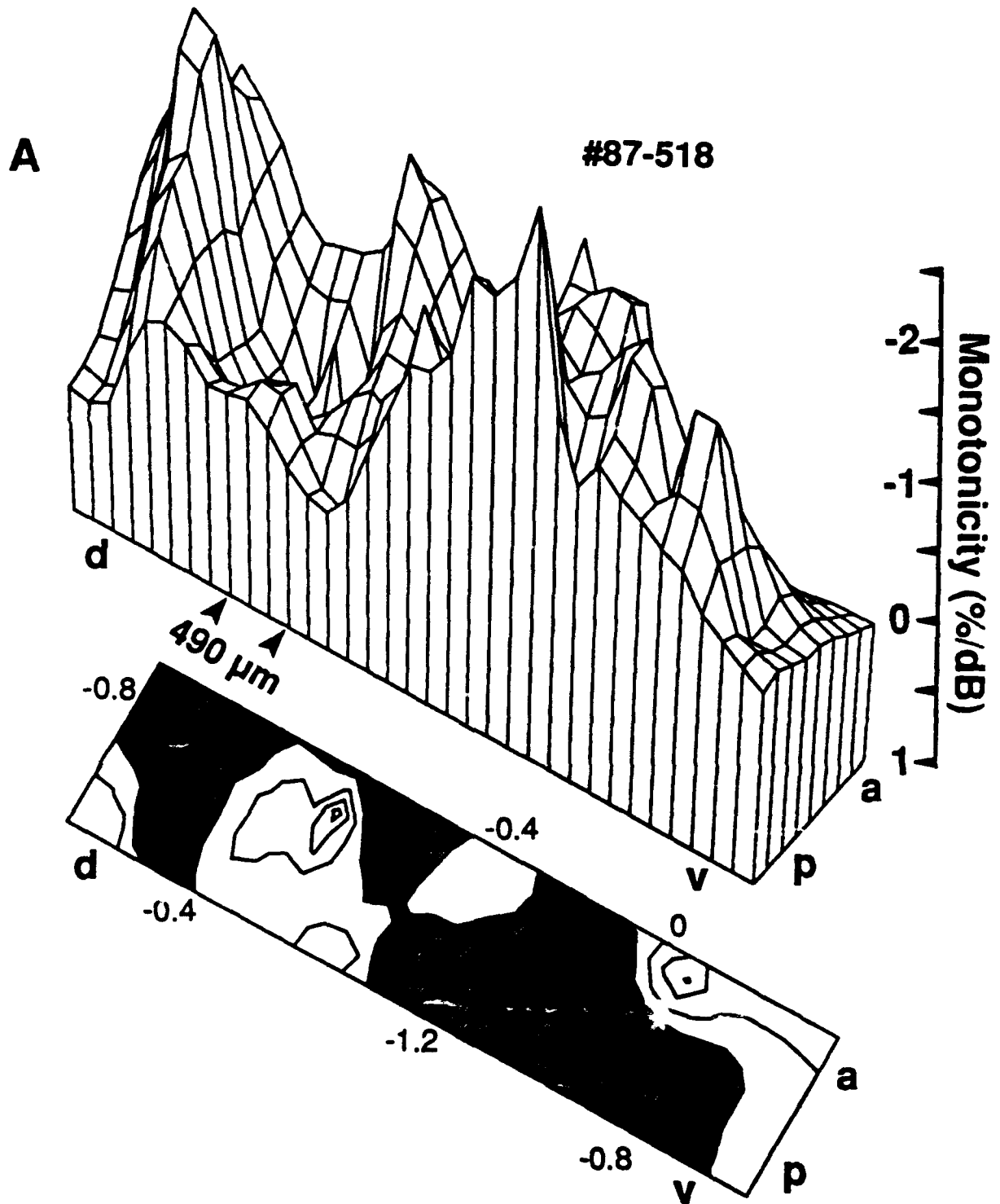


Figure 2: Spatial distribution of the degree of monotonicity encountered in AI expressed in %/dB. The upper portion depicts a pseudo three-dimensional projection of the spatial distribution of nonmonotonicity in AI (case #87-518). Note that negative values, i.e. the degree of nonmonotonicity, are proportional to the elevation of the grid surface. The lower portion of the panel shows an undistorted contour-plot representation of the same data. The contour intervals are 0.4 %/dB. Shaded areas correspond to nonmonotonicities below -0.4 %/dB. (See Fig. 1 for further details.)

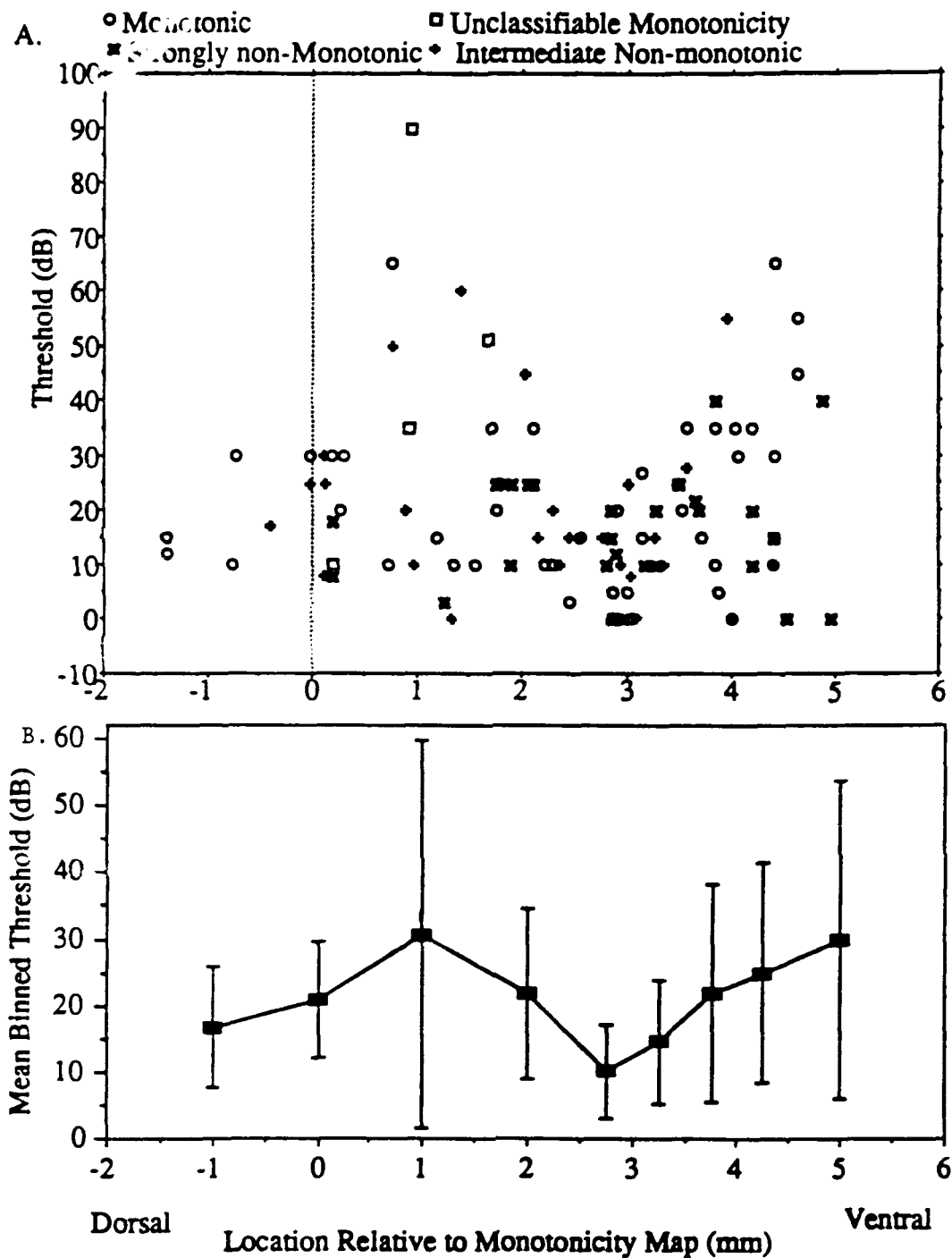
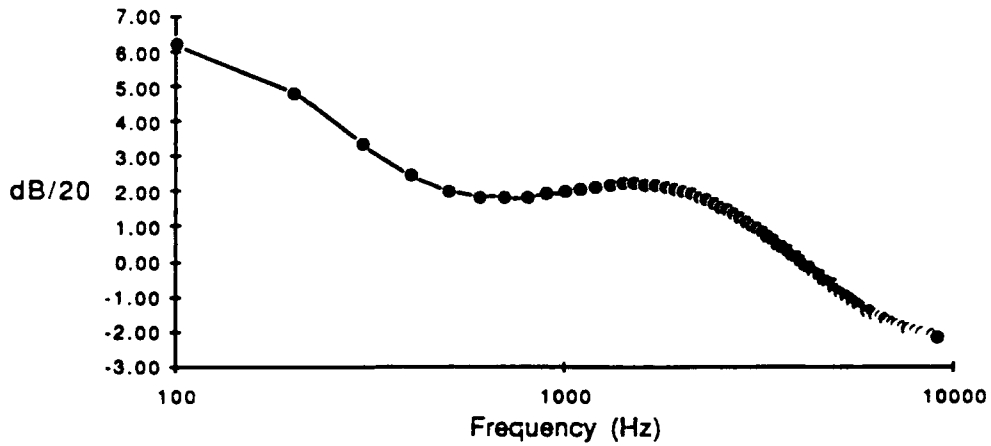


Figure 3. Threshold data pooled across animals. Zero and three millimeters correspond to two non-monotonic areas. Threshold was referenced such that for each animal 0 dB corresponded to the lowest multiple unit threshold encountered. Notice the minima in threshold scatter at the two non-monotonic areas and the threshold minimum at the ventral non-monotonic area.

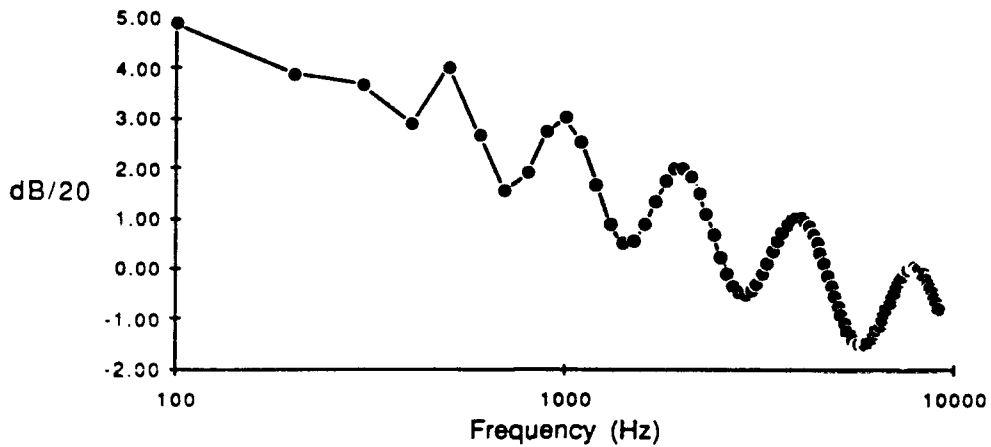
(A) Scatter plot of all neurons. Symbol legend in Figure.

(B) Mean binned threshold with standard deviation (error bars) to represent threshold scatter.

Ripple Spectrum (at 2 kHz: 0.25 rip/oct)



Ripple Spectrum (at 2kHz :1 rip/oct)



Ripple Spectrum (at 2kHz :4 rip/oct)

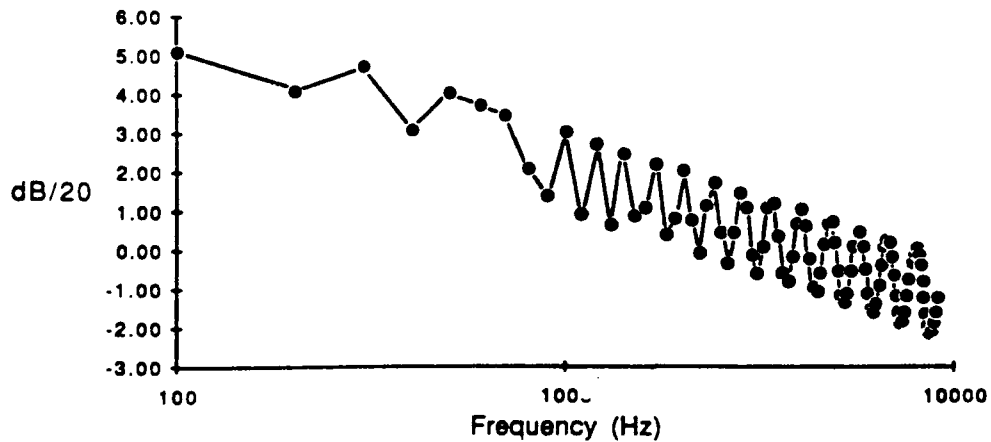
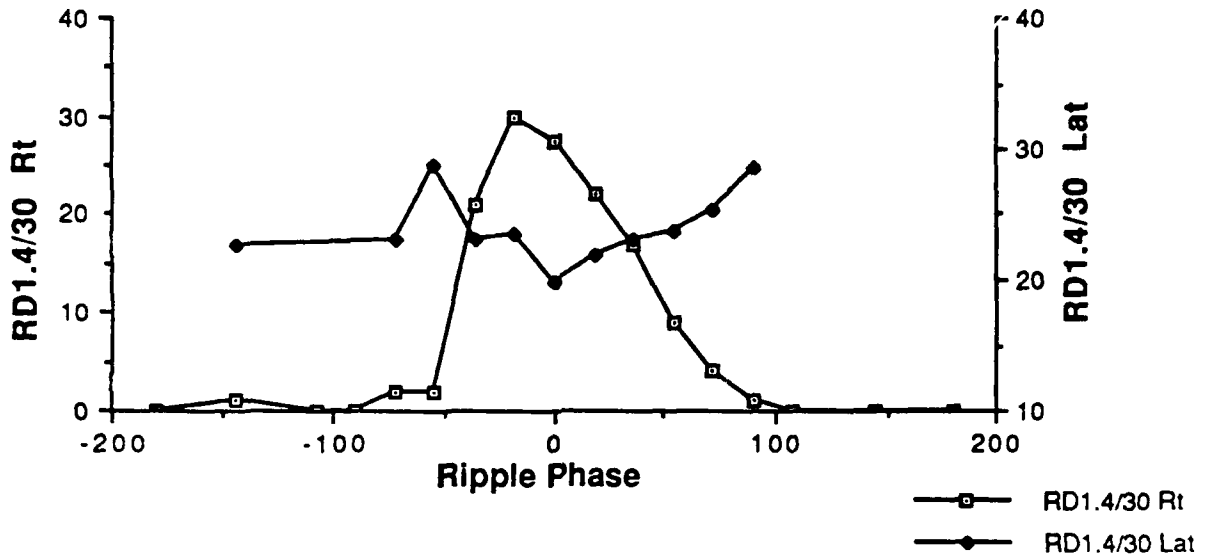


Fig. 4: Ripple spectra with three different ripple densities. Magnitude of each component is plotted as function of component frequency. The fundamental frequency of this harmonic complex is 100 Hz. Each dot corresponds to a single frequency component. The magnitude of the components is sinusoidally modulated in the logarithmic frequency domain. The number of relative maxima per octave gives the ripple density. A tilt of -6 dB/octave was introduced to keep the energy per octave a constant.

CH121.SU: Ripple Phase (-60 dB att.)



CH121.SU: Transfer function (-60 dB att; 30 dB Depth)

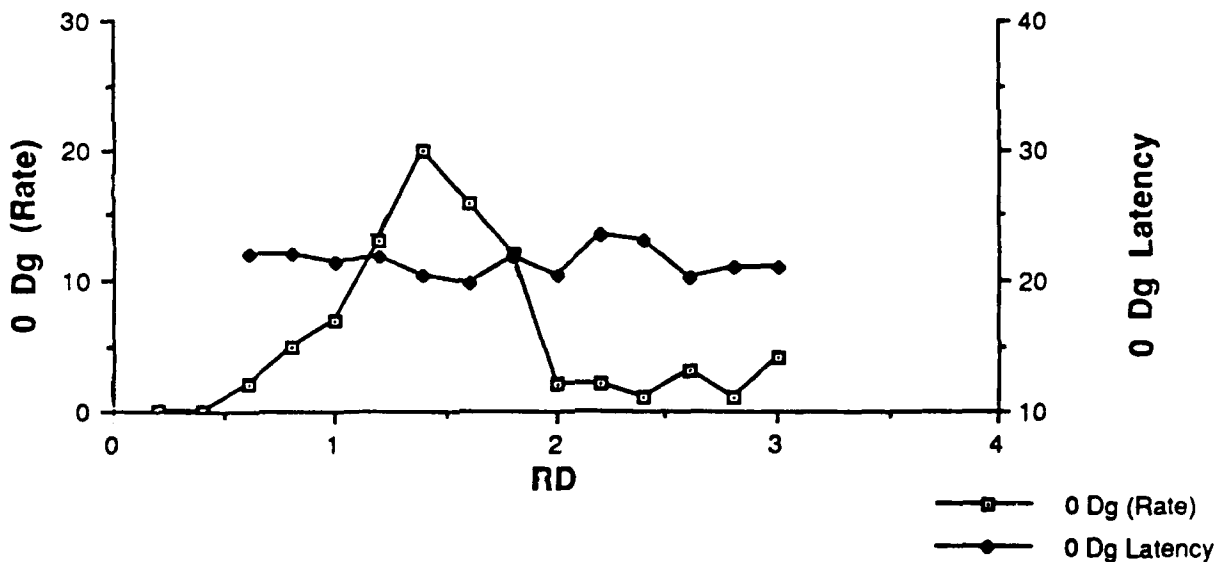


Fig. 5: Response of a single neuron in cat AI to variations of ripple phase and ripple density. (Pentobarbital anesthesia, recording depth 900 μm .) The upper panel plots the magnitude and the latency of the response to different ripple phases. The ripple density was 1.4/oct; ripple depth was 20 dB; the signal was 3 octaves wide centered at the CF of the neuron (9 kHz). The intensity of the signal was 25 dB above response threshold. The firing rate to 20 stimuli is plotted (left ordinate; open squares) as a function of ripple phase. The onset latency (closed diamonds, right ordinate) shows some variations with ripple phase. The lower panel depicts the ripple transfer function for the same neuron, i.e. the ripple density is the independent variable. Responses to 15 repetitions of each stimulus are plotted.

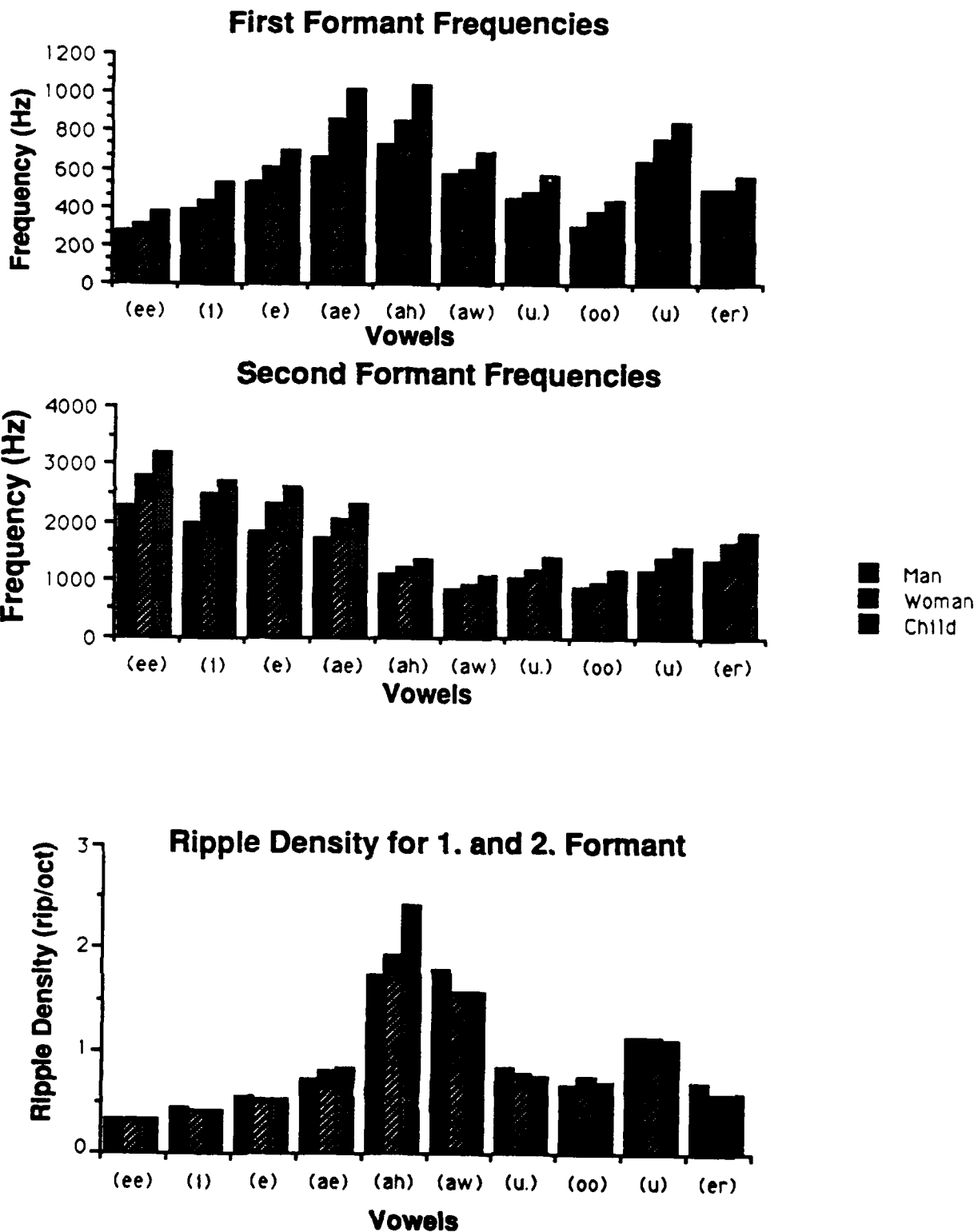


Fig. 6: Formant frequencies and ripple densities of english vowels. Upper panel: Average frequencies of first and second formants of adult male, adult female, and children. Lower panel: The ripple densities of the formant spacing between the first and second formant is plotted for english vowels. Note the speaker independence of the relative ripple density measure compared to the absolute frequency location measure.

Phase Plot for Ripple Density of 1 (1 subject)

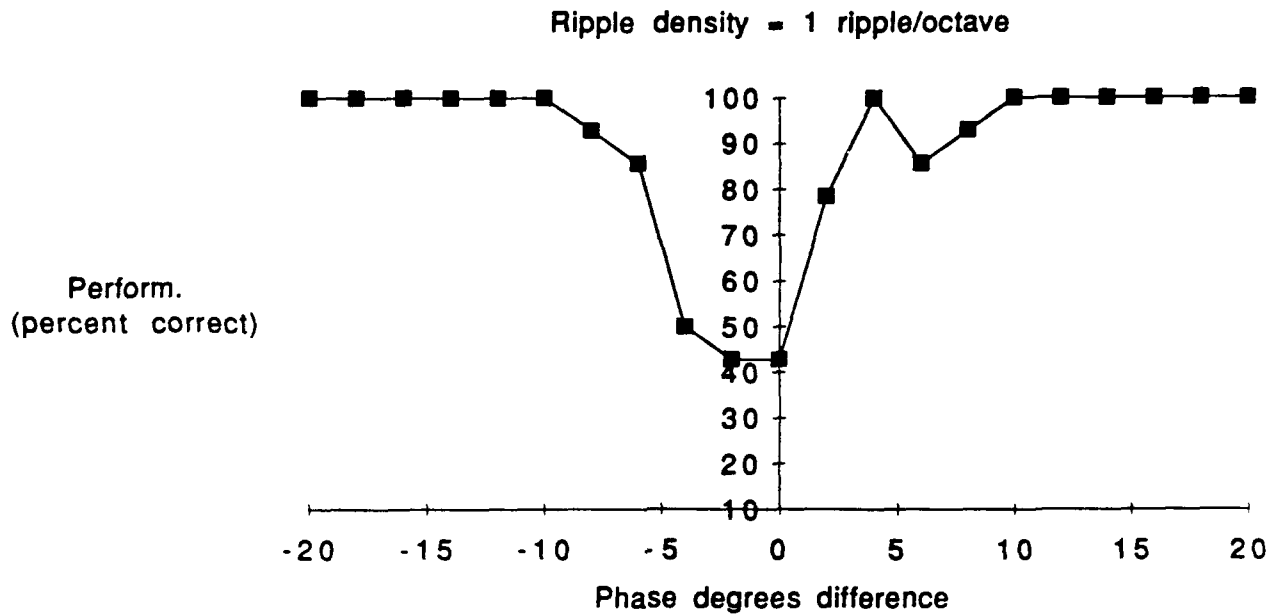


Fig. 7: Psychophysical estimate of ripple phase sensitivity in humans. A ripple stimulus with a fundamental frequency of 100 Hz, and a bandwidth of 3 octaves centered at 3 kHz was created. Roving levels around 40 ± 6 dBSL were used. Three stimuli were presented to the subject, who was wearing headphones, and seated in a sound-attenuated chamber. The first stimulus was a standard stimulus with a ripple density of 1 ripple/octave and ripple phase zero (i.e. the central ripple peak was located at 3 kHz); one of the next two stimuli was randomly varied in ripple phase in comparison to the standard within the range $+20$ to -20 degrees corresponding to maximal frequency shifts of the ripple maxima of $1/18$ of an octave. The subject was instructed to indicate which of the test stimuli was the odd (different) stimulus - stimulus 2 or stimulus 3 (constant stimulus, two alternative forced choice method). Performance was calculated as percent correct at each phase difference. There were 21 data points at each phase location within a trial session. Threshold for detection was considered as 75% correct. For this subject, detection thresholds were at 5.4 degrees (0.015 octaves) for shifts toward lower frequencies and 1.8 degrees (0.005 octaves) for shifts to higher frequencies.

Appendix A:

Manuscript:

Functional topography of cat primary auditory cortex: excitatory bandwidths of single neurons. By Christoph E. Schreiner and Mitchell L. Sutter.

Submitted to Journal of Neurophysiology.

Functional Topography of Cat Primary Auditory Cortex:
Excitatory Bandwidths of Single Neurons

CHRISTOPH E. SCHREINER and MITCHELL L. SUTTER

*Coleman Laboratory, Department of Otolaryngology, University of California, San Francisco,
San Francisco, CA 94143-0732, USA.*

Running Head: Topography of Excitatory Bandwidth in AI

Address to which correspondence should be sent:

Dr. Christoph Schreiner, Coleman Laboratory, UCSF, San Francisco, CA 94143-0732, USA.

SUMMARY AND CONCLUSION

1) The spatial distribution of the sharpness of tuning of single neurons along the isofrequency domain of primary auditory cortex (AI) was studied. The sharpness of tuning gradient was obtained with multiple unit recordings, and in combination with the cochleotopic organization, served as a frame of reference for the locations of single neurons. The frequency selectivity or 'integrated excitatory bandwidth' of multiple units varied systematically along isofrequency contours in AI. The most sharply tuned unit clusters were found at the approximate center of essentially dorso-ventrally oriented isofrequency contours. A gradual broadening of the integrated excitatory bandwidth in both dorsal and ventral directions was consistently seen.

2) The multiple unit measures of the bandwidth 10 dB (BW10) and 40 dB (BW40) above minimum threshold, pooled across several animals and expressed in octaves, were similar to those described within individual cases in cats. As in the individual animals, the bandwidth maps were V-shaped with minima located at the approximate center of the dorsal-ventral extent of isofrequency contours in AI. The location of the minimum in the multiple unit bandwidth map (i.e. the most sharply tuned area) was used as a reference point to pool single neuron data across animals.

3) For single neurons, the dorsal half of the BW40 distribution showed a gradient paralleling that of multiple units. For both single and multiple units, the average excitatory bandwidth increased at a rate of approximately 0.27 octaves per millimeter from the center of AI toward the dorsal fringe. Differing from the dorsal half of AI, the ventral half of AI showed no clear BW40 gradient for single units along its dorso-ventral extent. At 40 dB above minimum threshold, most ventral neurons encountered were sharply tuned. By contrast, the multiple unit BW40 showed a gradient similar to the dorsal half with 0.23 octaves per millimeter increasing from the center toward the ventral border of AI.

4) For single neurons, BW10 showed no clear systematic spatial distribution in AI. Neither the dorsal nor the ventral gradient was significantly different from zero slope although the dorsal half showed a trend toward increasing BW10s. Contrasting single neurons, both dorsal and ventral halves of AI showed BW10 slopes for multiple units confirming a V-shaped map of the integrated excitatory bandwidth within the isofrequency domain.

5) Based on the distribution of the integrated (multiple unit) excitatory bandwidth, AI was parceled into

three regions: the dorsal gradient, the ventral gradient, and the central narrowly tuned area. In ventral AI, single units were significantly more sharply tuned than multiple units for BW10 and BW40. In dorsal AI, single units were not statistically different from multiple units for BW40. In central AI, single units were significantly sharper for BW40, but not BW10.

6) Estimates of the scatter of best frequency (BF) of single neurons in the isofrequency domain were obtained relative to the frequency organization determined with multiple units. The central narrowly tuned region showed the least BF scatter. The BF scatter increased toward the dorsal, and in particular, the ventral end of the isofrequency domain.

7) The combined single and multiple unit results suggest that AI is composed of at least two functionally distinct sub-regions along the isofrequency domain based on the bandwidth properties of tuning curves. The dorsal region (AId) displays a gradient of BW40 expressed in single and multiple unit measurements, and contains broadly and sharply tuned single-peaked as well as multi-peaked neurons. The ventral region (AIv) predominantly contains neurons narrowly tuned at 40 dB above threshold. The increase in integrated (multiple-unit) excitatory bandwidth in AIv can be related to a progressively larger BF scatter at more ventral locations. The transition between AId and AIv is delineated by a reversal in the BW40 gradient for multiple units coinciding with a region of small BF scatter of the underlying single neurons.

INTRODUCTION

Recent studies of cat auditory cortex have demonstrated topographic order within the electrophysiologically determined organization of the isofrequency domain of the primary auditory cortical field (AI) (Schreiner and Cynader 1984; Schreiner et al. 1988, Mendelson et al. 1988, Schreiner and Mendelson 1990; Sutter and Schreiner 1991a) that goes beyond previously described binaural response organizations (Imig and Adrian 1979; Middlebrooks et al. 1980; Reale and Kettner 1986). Several response parameters, including sharpness of frequency and amplitude tuning, obtained from multiple unit recordings, were found to be nonrandomly distributed along the dorso-ventral dimension of AI. These findings suggest a systematic functional organization in the isofrequency domain of AI that involves the coding of basic signal properties, among them signal intensity and spectral complexity (Schreiner and Mendelson 1990, Sutter and Schreiner 1991a, Shamma and Fleshman 1990). The functional interpretation of topographies based on multiple unit recordings is, however, limited and can only represent an approximation of actual cortical processing. Ultimately, the properties of single neurons underlying those integrated measures of cortical activity must be analyzed and related to multiple unit findings in order to better understand the basic principles of the physiological and functional organization of AI.

Studying the spatial distribution of single neuron response properties across large portions of AI has proven to be a difficult task for a number of reasons. Historically, single unit studies that used anatomically based pooling strategies (e.g., Evans and Whitfield 1964, Goldstein et al. 1970) failed to fully support basic organizational principles such as a strong cochleotopicity of AI as obtained with integrated measures. For example, using sulcal patterns and vasculature as landmarks for pooling topographical data across animals is untenable since both display a large variability between animals (Merzenich et al. 1975). Additionally, the cytoarchitectonic boundaries of AI are not sharply expressed enough (e.g., Rose 1949, Winer 1984) to guide a precise alignment of individual fields and their functional organizations. Characterizing a sufficient number of single neurons in one experiment in order to construct a reliable physiological map is difficult in a cortical field of the extent of cat AI.

An alternative to utilizing anatomical landmarks is the use of known systematic spatial distributions of physiological features that may provide information for the proper spatial alignment of

fields from several individual cortices. The most basic choice is the use of the cochleotopic frequency gradient, reliably determinable with multiple unit recordings (e.g. Merzenich et al. 1975, Reale and Imig 1980, Schreiner and Mendelson 1990), to determine the rostro-caudal extent of the field and to identify locations within this dimension. However, a second parameter is necessary to align locations along the dorso-ventral extent of AI, i.e. approximately along its isofrequency domain, since the clustered distribution of binaural response characteristics along the dorso-ventral extent of AI is quite variable from animal to animal (Imig and Adrian 1979, Imig and Brugge 1978, Imig and Reale 1981, Middlebrooks et al. 1980, Reale and Kettner 1986, Schreiner and Cynader 1984) and, therefore, seems not to be suitable as a basis for a spatial normalization or alignment of AI from different cortices.

A second physiological parameter that may be particularly useful in aligning cortical fields is the spatial distribution of the integrative excitatory bandwidth along the dorso-ventral dimension of AI. A recent study (Schreiner and Mendelson 1990) revealed a region of sharp frequency tuning of multiple unit responses within the central isofrequency domain contiguous with ventral and dorsal gradients of decreasing frequency selectivity. This spatial distribution of the integrated excitatory bandwidth in AI (Schreiner and Cynader 1984, Schreiner and Mendelson 1990) appears to be similar from animal to animal and may serve as a topographical frame of reference for comparing and pooling data from different animals. In a previous report, this approach was successfully utilized to determine the spatial distribution of a subpopulation of auditory cortical neurons, namely neurons with multi-peaked tuning curves, in the dorso-ventral dimension of AI (Sutter and Schreiner 1991a). By pooling data across animals, a sufficient number of topographically identifiable neurons with multi-peaked tuning curves was obtained to derive a statistically secured estimation that their locations were essentially confined to the dorsal part of AI. This paper explores the property and topography of frequency selectivity of single neuron responses along the dorso-ventral extent, approximating the isofrequency axis of cat AI. Single neuron positions were obtained relative to gradients in integrated excitatory bandwidth determined with multiple unit recordings. Some results have previously been presented in abstract form (Sutter and Schreiner, 1991b).

METHOD

Surgical Preparation

The methods are similar to those described in Sutter and Schreiner (1991a). Experiments were conducted on 9 young adult cats. Anesthesia was induced with an intramuscular injection of ketamine hydrochloride (10mg/kg) and acetylpromazine maleate (0.28 mg/kg). After venous cannulation, an initial dose of sodium pentobarbital (to effect, approximately 30 mg/kg) was administered. Animals were maintained at a surgical level of anesthesia with a continuous infusion of sodium pentobarbital (2 mg/kg per hour) in lactated Ringer's solution (infusion volume: 3.5 ml/hour) and, if necessary, with supplementary intravenous injections of sodium pentobarbital. The cats were also given dexamethasone sodium phosphate (0.14 mg/kg, IM) to prevent brain edema, and atropine sulfate (1 mg, IM) to reduce salivation. The temperature of the animals was recorded with a rectal temperature probe and maintained at 37.5° C by means of a heated water blanket with feedback control.

The head was fixed, leaving the external meati unobstructed. The temporal muscle over the right hemisphere was then retracted and the lateral cortex exposed by a craniotomy. The dura overlaying the middle ectosylvian gyrus was removed, the cortex was covered with silicone oil, and a photograph of the surface vasculature was taken to record the electrode penetration sites. For recording topographically identified single neurons, a wire mesh was placed over the craniotomy and the space between the grid and cortex was filled with a 1% solution of clear agarose. This approach diminished pulsations of the cortex and provided a fairly unobstructed view of identifiable locations across the exposed cortical surface.

Stimulus Generation and Delivery

Experiments were conducted in a double-walled sound-shielded room (IAC). Auditory stimuli were presented via calibrated headphones (STAX 54) enclosed in small chambers that were connected to sound delivery tubes sealed into the acoustic meati [Sokolich 1981, U.S Patent 4251686]. The sound delivery system was calibrated with a sound level meter (Brüel & Kjaer 2209) and a waveform analyzer (General Radio 1521-B). The frequency response of the system was essentially flat up to 14

kHz and did not have major resonances deviating more than ± 6 dB from the average level. Above 14 kHz, the output rolled off at a rate of 10 dB/octave. Harmonic distortion was at least 55 dB below the primary (depending on the sampling rate and the settings of the antialiasing low-pass filter.)

Tones were generated by a microprocessor (TMS32010; 16 bit D/A converter at 120 kHz sampling rate; low-pass filter of 96 dB/octave at 15, 35 or 50 kHz). The processor-related useful dynamic range of these stimuli was <78 dB, allowing a 3-bit amplitude resolution at the lowest used level. Additional attenuation was provided by a pair of passive attenuators (Hewlett Packard). The duration of the tone bursts was usually 50 ms (tone bursts were extended to 85 msec for long-latency responses) including 3 ms rise/fall time. The interstimulus interval was 400 to 1000 ms.

Frequency Response Areas

Frequency response areas (FRAs) were obtained for each neuron. To generate an FRA, at least 675 different tone bursts were delivered. Tone bursts were presented in a pseudorandom sequence of different frequency/level combinations selected from 15 level values and 45 frequency values. Steps between levels were 5 dB, resulting in a sampled dynamic range of 75 dB. Occasionally higher resolution FRAs were recorded with 2700 (30 levels by 90 frequencies) different tones.

The frequency range covered by the 45 frequency steps was centered around the estimated best frequency (BF) of the recording site and covered between 2 and 5 octaves, depending on the width of the frequency tuning curve as obtained by audio-visual criteria. Stimulus frequencies were chosen so that the 45 presented frequencies were spaced an equal fraction of an octave over the entire range (for most cases this provided an 0.067 octave resolution over a total of 3 octaves).

Recording Procedure

Parylene-coated tungsten microelectrodes (Microprobe Inc.) with impedances of 1.0-8.5 MOhm at 1 kHz were introduced into the auditory cortex with a hydraulic microdrive (KOPF) remotely controlled by a stepping motor. All penetrations were essentially orthogonal to the brain surface. The recordings reported here were derived at intracortical depths ranging from 600 to 1000 μ m as determined by the microdrive setting, roughly corresponding to portions of cortical layers 3 and 4.

Neuronal activity of single neurons, and for the initial mapping, small groups of neurons were amplified, band pass filtered, and monitored on an oscilloscope and an audio monitor. Action potentials were isolated from the background noise with a window discriminator (BAK DIS-1). The number of spikes per presentation and the arrival time of the first spike after the onset of the stimulus were recorded and stored in a computer (DEC 11/73). The recording window had a duration of 50 to 85 ms, corresponding to the stimulus duration and excluding any offset responses.

Data Analysis

From the responses to 675 different frequency/level combinations, an objectively determined frequency response area (FRA) was constructed for every neuron or group of neurons. Figure 1 shows an example of 3 reconstructed FRAs obtained in AI. The ordinate corresponds to the sound level of the tone-burst stimulus, while the abscissa corresponds to the frequency. All presented stimuli would be represented by a 15 (ordinate) by 45 (abscissa) grid with equal spacing and size of elements. Responses are represented at the point of intersection of the intensity and frequency of each presented stimulus. The length of the line at each intersection is proportional to the number of spikes discharged in response to the stimulus. The absence of a line for a given point of stimulus presentation represents no response. Usually each stimulus was presented once. If the resulting FRA was not well defined, the process was repeated with the same 675 stimuli and the resulting evoked activity was added to the first set of responses.

A tuning curve was extracted from the FRA using an objective method. For the response threshold, a computer program defined the iso-response criteria as the spontaneous rate (estimated from 45 points outside the response area) plus 20% of the peak rate (9 point weighted averaging). Weighted 9 point smoothing/averaging was used to determine the response of each point. This criterion was robust, yielding comparable tuning curves for the wide range of FRAs recorded, including high spontaneous multiple unit and low spontaneous single unit recordings. Shaded areas in Figure 1 correspond to the calculated FRAs. From these objectively determined single tone tuning curves several response properties were measured. Among them were a) the best frequency (BF) (the stimulus frequency with the lowest sound pressure level necessary to evoke neuronal activity); b)

BW10 (the bandwidth of the frequency response area, in octaves, 10 dB above minimum threshold), and c) BW40 (the bandwidth of the frequency tuning curve, in octaves, 40 dB above minimum threshold).

For units with multi-peaked tuning curves the entire response area including the non-responsive area between individual peaks was used to determine the excitatory bandwidth.

RESULTS

Results are based on a total of 146 multiple units and 103 single neurons from 9 cats. On the average, multiple unit maps were derived from approximately 15 fairly evenly spaced recording locations over a restricted BF range (usually < 2 octaves). From the multiple unit recordings, three parameters were extracted. First, the AI/AII border was determined in accordance with criteria suggested by Schreiner and Cynader (1984). The criteria for AII are based on a reliable and spatially consistent shift of three multiple unit physiological properties: (1) an increase in thresholds by 15dB or more, (2) Q-10dB values (BF/excitatory bandwidth 10 dB above minimum threshold) below a certain BF-dependent value, and (3) a blurring of the BF topography. Single neurons falling into AII were not included in the analyzed set of data. Second, the orientation of the isofrequency gradient within AI was determined, and third, the distribution of the integrated excitatory bandwidth 10 and 40 dB above minimum threshold was reconstructed. Usually, responses to pure tones could not be recorded more dorsal than 2 millimeters ventral to the suprasylvian sulcus. In a few cases, neurons with responses to pure tones were recorded as close as 1.0 mm from the suprasylvian sulcus.

A large range of bandwidths for multiple and single units were encountered in this series of experiments corresponding to ranges seen for Q-10dB and Q40-dB for multiple units in previous experiments (Schreiner and Mendelson 1990), as well as for Q-10dB (Phillips and Irvine 1981) and bandwidth values (Hind 1960; Abeles and Goldstein 1970a,b) for single neurons. Figure 1 displays typical examples of FRAs with sharp, medium and broad frequency tuning of single neuron responses. Bandwidth measures BW10 and BW40 for the units are indicated.

Topography of Integrated Excitatory Bandwidth

To topographically characterize the dorso-ventral axis of AI, electrode penetrations orthogonal to the cortical surface were placed in close approximation to the orientation of isofrequency contours. For most of AI, isofrequency contours could be fitted with a straight line deviating slightly from the dorsal-ventral direction with the dorsal end slanting posteriorly. The angle between the orientation of the approximated course of an isofrequency contour could deviate as much as 30 degrees from the dorso-ventral axis. The BF topography became weaker at the most dorsal extent of the ectosylvian gyrus where isofrequency contours often slanted even more posteriorly (Middlebrooks and Zook 1983, Sutter and Schreiner 1991a). Cortical recording locations are represented as dorso-ventral distance along the approximated orientation of the straight portion of isofrequency contours. The range of BFs included for each case varied between 0.2 to 3 octaves. All locations included in the current data evaluation had BFs larger than 4 kHz. The actual BFs used to create a map are illustrated for one case (see Figure 3). In contrast to most previous studies, the sharpness of frequency tuning in this study was measured as bandwidth expressed in octaves. Similar to the traditionally used Q-factor (BF/bandwidth), the bandwidth measure is essentially frequency independent and has the additional advantage of being independent from the location of the BF within the FRA, i.e. it is not influenced by the symmetry of the FRA or tuning curve.

The spatial distribution of the integrated excitatory bandwidths for pure tones obtained in this study was consistent with that of previous reports (Schreiner and Mendelson 1990, Sutter and Schreiner 1991a). Locations with sharply tuned multiple-unit responses yielding a narrow integrated excitatory bandwidth were found in a region near the dorso-ventral center of the straight segment of isofrequency contours 1.5 to 3 mm dorsal to the AI/AII border. Locations dorsal and ventral to this point gradually showed more broadly tuned responses.

Figure 2 illustrates multiple unit bandwidth maps obtained 10 and 40 dB above minimum response threshold for two representative individual cases. Panels A and B show the reconstructed BW40 maps. Circles connected by dotted lines show the actual bandwidth values. These and other cases show a distinct bandwidth minimum surrounded by areas with broader frequency tuning. Case SUTC16 (right panels) showed a larger variability in sharpness of tuning in areas that contained, on

the average, wider bandwidths. The dorso-ventral progression of bandwidth changes was much smoother in case SUTC12 (left panels). To aid in demarcating the minima of bandwidth plots, a 500 micron, spatially weighted smoothing algorithm was used (100% smoothing for points at the same cortical distance to no weighting for points more than 500 microns apart). The smoothed version of the BW40 maps are shown as solid lines in Figures 2 A and B, respectively. Arrows point to the location of the main minimum in each bandwidth function. The data points and the smoothed version of the BW10 map for these two cases are shown in Figure 2 C and D. In both cases, the BW10 minima are located 0.5 to 1 mm dorsal to the BW40 minimum in agreement with previous findings for Q-10dB and Q-40dB (Schreiner and Mendelson, 1990). The minima of these functions ($BW10_{\min}$ and $BW40_{\min}$) served as physiological reference points to spatially pool excitatory bandwidth data across animals.

Single Neuron Maps

The spatial distribution of excitatory bandwidths for single neurons and multiple units is shown in Fig. 3 for case SUTC16. For this animal, a sufficient number ($N=27$) of single neurons were sampled to directly compare single and multiple unit topographies within the same animal. The origin of the abscissa designates the location of the combined bandwidth minimum, that is, the averaged location of the BW10 and BW40 minima. For BW40 (Fig. 3A), the spatial distribution of the single neuron sharpness was quite similar to the integrative excitatory bandwidth. Neurons with the narrowest bandwidth were located at or near the multiple unit bandwidth minimum. Dorsal to the minimum, the bandwidth for single neurons increased and showed a scatter similar to that expressed in the multiple-unit responses. Ventrally, the excitatory bandwidth of single neurons also increased progressively. However, sharply tuned neurons were found throughout the ventral region of AI and, overall, the range and scatter of the integrated excitatory bandwidth appeared to be larger than for the single neuron bandwidth. The distribution of BW10 values for single and multiple units (Fig. 3B) were also fairly similar. In this particular case, the minimum of the bandwidth distribution was not very strongly expressed for either multiple (see Fig.2D) or single neurons. However, the apparent scatter of encountered bandwidths appeared to be the smallest near the estimated center of the

bandwidth distribution. The BFs of the single neurons are shown at the corresponding bandwidth values in Fig. 3 C and D. The BFs covered a range of about one octave and did not show a strong influence on the bandwidth distributions (see Discussion).

Pooling Relative to Multiple Unit Maps

The reconstruction of the spatial bandwidth distribution for case SUTC 16 was made possible by sampling a relatively large number of single (27) and multiple (28) units in the same experiment. This, however, was an exceptional case, and therefore, a method of pooling data across animals was necessary to generally assess the topography of single neuron characteristics.

In this study, the location of single neurons within an experiment was referenced relative to the multiple unit bandwidth map. The alignment and pooling procedure is illustrated in Fig. 4 for the two cases shown in Figs. 2 and 3. To aid in visualizing this procedure, single neurons from case SUTC12 are marked by filled diamonds and single neurons from case SUTC16 are marked by crosses. The unsmoothed BW40 maps for cases SUTC12 and SUTC16 (from Figs. 2 A and B) are represented by open circles connected by lines in Fig. 4 A and B. For these two experiments, the dorsal-ventral extent of AI was approximately 6.2 and 5.3 mm, respectively. To pool data across these two experiments, the minimum in the smoothed BW40 distribution ($BW40_{\min}$ marked by arrows) was assigned the reference value of zero millimeters and the positions of all recording points were expressed as distance in millimeters from $BW40_{\min}$. Next, the $BW40_{\min}$ of all cases was aligned. The shifted and aligned recording locations of the two cases are shown in Fig. 4 C and D. Finally, the locations of single neurons were pooled across both aligned maps as displayed in Fig. 4 E. No distance normalization or distortion of the individual recording locations is involved in this method and, accordingly, the pooled data reflect the trends discernible in each individual case. This procedure was used to pool data across all 9 cases.

BW40 Topography

Scattergrams of BW40 values for all pooled single and multiple units are shown in Figs. 5 A

and B. Cortical locations were aligned relative to $BW40_{\min}$ for each individual case as described above. For multiple-unit responses, the pooled BW40 data show the same pattern seen in individual cases in this and previous studies (Schreiner and Mendelson 1990, Sutter and Schreiner 1991a). In particular, a region of sharp tuning, located at the approximate dorso-ventral center of AI, was aligned with integrated excitatory bandwidths that gradually increased with increasing distance.

The pooled distribution of BW40 for single neurons (Fig. 5B) shows some similarities and some dissimilarities to the multiple-unit distribution. Dorsal to the BW40 minimum, single units show the same tendency of increasing bandwidth with dorsal distance as seen with multiple units. Partially responsible for this overall increase in bandwidth is the occurrence of multi-peaked FRAs in the dorsal aspect of AI (crosses in Fig. 5B) in accordance with a previous report of their spatial distribution (Sutter and Schreiner 1991a). Single-peaked FRAs in dorsal AI also tended to have broader tuning. However, some sharply tuned single and multiple neuron responses can be found across the entire dorsal half of AI or at least up to 3 mm dorsal to the bandwidth minimum.

In the AI portion ventral to the bandwidth minimum, the pooled single neuron data deviated from the trend seen in multiple unit recordings as well as from that seen in the single neuron example shown above (Fig. 3): BW40 of almost all ventral single neurons remained essentially sharply tuned (below 0.7 octaves) independent of their location in ventral AI. By contrast, the multiple unit recordings showed increasing bandwidths with distance from the BW minimum. The location of the AI/AII border varied from 1.65 to 3.45 millimeters from $BW40_{\min}$ and no single neurons located within AII were included. However, even locations as close as 1 mm ventral to the BW40 minimum, and therefore located well within AI, showed multiple unit locations with bandwidths in excess of one octave whereas all ventral single neurons remained below that value. Figure 5C shows a direct comparison of the single and multiple unit scattergrams. BW40 values were binned and averaged over 500 microns. The mean BW40 values of multiple (shaded columns) and single (solid columns) units are shown. Standard deviations are represented by error bars. The mean and standard deviation of BW40 increased gradually toward the dorsal end of AI for multiple and single units. Ventrally, mean and standard deviation of BW40 for single neurons remained constant whereas the multiple unit values increased toward and into AII.

The gradients of the bandwidth progressions dorsal and ventral to the bandwidth minimum can be approximated by regression lines as is shown by the dashed lines in Figure 5A and 5B. For the dorsal portion of the multiple unit distribution, the regression line is described by $y = -0.25x + 0.42$ ($r = 0.49$). The slope of the dorsal gradient is -0.25 oct/mm. The 95% confidence interval of the slope lies between -0.14 and -0.38 oct/mm. The regression line of the ventral multiple unit BW40 gradient was $y = 0.23x + 0.47$ ($r = 0.38$). The slope, 0.23 oct/mm, is similar but slightly less than that of the dorsal gradient. The larger scatter on the ventral side is reflected in a 95% confidence interval containing slopes between 0.09 and 0.36 oct/mm. For both sides of the distribution, the zero slope lies outside of the 99.5% confidence intervals. Therefore, it is concluded that the multiple unit BW40 distribution along the isofrequency axis of AI is concave with a minimum ('V-shaped').

Contrasting the multiple unit distribution, the single unit topography (Fig. 5B) appeared to be essentially flat on the ventral side. The slope of the regression line ($y = 0.05x + 0.28$; $r = 0.03$) was 0.05 oct/mm. The 95% confidence intervals comprise slopes between -0.04 and 0.13 oct/mm which includes zero slope. Therefore, it cannot be claimed with 95% confidence, that the slope is greater than zero. Dorsally, the slope of the average excitatory bandwidth was -0.28 oct/mm ($y = -0.28x + 0.28$; $r = 0.48$; 95% confidence interval: -0.13 to -0.42 oct/mm), that is, similar to the dorsal slope obtained for multiple units.

Parceling of AI: Regional Differences in BW40

In order to test the hypothesis that the isofrequency domain of AI may consist of more than one physiologically distinguishable region, AI was subdivided into three regions based on the bandwidth distribution: one millimeter to each side of the location of minimum bandwidth was arbitrarily defined as the 'central' region of AI; dorsal and ventral to this area were defined correspondingly. The minimum bandwidth measure used to pool data for this analysis was the location of $BW40_{\min}$ and $BW10_{\min}$ averaged for each particular case (BW_{\min}). This measure was used so that the same topographical parceling can be performed without biasing toward either bandwidth measure. Figure 6 shows the histograms of BW40 for the dorsal, ventral and central regions of AI for single (black bars) and multiple (shaded bars) units. Median values for the histograms are summarized in Fig. 6C.

Deviation bars represent one half of the 75th percentile BW value minus the 25th percentile value.

Table 1 lists the mean BW40 values found with single and multiple unit recordings. A significant difference between the BW40 distributions of multiple and single units in the ventral and central parts of AI was established (non-parametric Mann-Whitney U test, $p < 0.01$, see Table 2). In dorsal AI, no significant difference was found ($p > 0.05$).

Analysis of variance (ANOVA) was applied to test for differences in bandwidth values of the three regions. Significant differences ($p < 0.01$) between regions were found for both single and multiple unit BW40 values (Table 3). Post-hoc Scheffe analysis showed that the ANOVA results for multiple units were due to differences between the central and ventral regions as well as between central and dorsal differences for multiple units. For single units, ANOVA differences could be accounted for by dorsal vs. central and dorsal vs. ventral regional differences. Non-parametric Mann-Whitney U tests confirmed the Scheffe results.

BW10 Topography

In contrast to BW40, the bandwidth or Q-value 10 dB above minimum threshold is not the most appropriate measure for a functionally highly relevant description of sharpness of frequency tuning of single cortical neurons (Suga and Manabe 1982, Suga and Tsuzuki 1985). However, since this measure has been almost exclusively used in cortical studies of species other than bats and since it does show systematic spatial variations in multiple unit recordings (Schreiner and Mendelson 1990, Sutter and Schreiner 1991), it was analyzed here as well to allow comparisons with other studies.

Scattergrams of BW10 for single and multiple units are shown in Fig. 7. Locations were pooled such that $BW10_{\min}$ was assigned the distance reference value of zero for each case. While the multiple unit distribution appeared to be V-shaped, paralleling the multiple unit BW40 distribution, such an effect appeared to be less pronounced in the distribution of BW10 for single neurons. For both, multiple and single unit recordings, FRAs narrowly tuned 10 dB above minimum threshold were encountered throughout the entire dorso-ventral dimension of AI. Dorsal to the bandwidth minimum, the slope of the regression line was -0.10 oct/mm (dashed line; $y = -0.10x + 0.14$; $r = 0.5$; 95% confidence interval: -0.06 to -1.15 oct/mm) for multiple units. Ventrally, the slope was 0.11 oct/mm

($y=0.11x+0.16$; $r=0.37$; 95% confidence interval: 0.05 to 0.18 oct/mm). For both dorsal and ventral halves, zero slope fell outside of the 99.5% confidence interval indicating that the distribution is V-shaped with 99.5% confidence, and thus, is similar to the BW40 distribution.

Regression analysis of single unit BW10 topography (dashed lines in Fig. 7B) did not show slopes significantly different from zero either dorsally or ventrally. Dorsally, the slope was -0.03 oct/mm ($y=-0.03x+0.19$; $r=0.14$; 95% confidence interval: -0.08 to 0.02 oct/mm). Ventrally, the gradient was 0.01 oct/mm ($y=0.01x+0.16$; $r=0.06$; 95% confidence interval: -0.04 and 0.06 oct/mm). It is concluded that the sharpness of frequency tuning 10 dB above minimum threshold does not change systematically for single neurons across the dorso-ventral extent of AI.

Parceling of AI: Regional Differences in BW10

For BW10, AI was parceled as described for BW40. Histograms are shown for single (Fig. 8A, black bars) and multiple (Fig. 8B, shaded bars) units in dorsal, central and ventral AI. The summary histogram of medians is shown in Fig. 8C. The mean BW10 values for the three regions are given in Table 1. There was a significant difference between BW10 for single and multiple units in the ventral ($p < 0.01$) and dorsal ($p < 0.05$) regions of AI (see Table 2). Centrally, there was no significant difference for BW10 between single and multiple units ($p > 0.05$).

For multiple units, ANOVA revealed significant differences between dorsal, ventral and central regions (Table 3). Scheffe post-hoc tests showed the significant ANOVA was due to differences between the dorsal and central region and between the central and ventral region. Mann-Whitney U tests confirmed the Scheffe results (Table 2). For single units, ANOVA (confirmed by Kruskal-Wallis test) showed no significant differences in BW10 between central, ventral and dorsal regions in AI (Table 3).

DISCUSSION

In this series of experiments, the bandwidth of FRAs 10 and 40 dB above minimum response threshold was used to investigate a) whether pooling of data across animals can be successfully used to reveal physiological topographies, and b) how single neuron response properties relate to

physiological gradients obtained with multiple-unit recording techniques. The main findings of this study can be summarized as follows: 1) Multiple-unit bandwidth data, pooled along the isofrequency-domain of AI, reflect the same spatial distribution as previously seen in individual cases (Schreiner and Mendelson 1990), namely, a region approximately 1.5 to 3 mm dorsal to the AII border contained narrow integrated excitatory bandwidths gradually giving way to more broadly tuned responses dorsally as well as ventrally. 2) Excitatory bandwidths of single neurons, pooled relative to the multiple-unit bandwidth topography, significantly differed from the multiple-unit distribution in the region of AI ventral to the bandwidth minimum, that is, no clear gradient in sharpness of single neuron responses was evident for either BW10 or BW40; in the region of AI dorsal to the minimum in multiple unit bandwidth, a spatial gradient and increasing variance was evident for the BW40 of single neurons similar to the one obtained for multiple units, however, no clear gradient was apparent for BW10 of single neurons.

Methodological Considerations

Before discussing some implications of these findings, a brief look at the pooling method is in order. Single and multiple unit properties were pooled along an approximation of the isofrequency axis of AI, nearly corresponding to a line with dorso-ventral orientation. The location of the minimum in multiple-unit bandwidth either 10 or 40 dB above minimum response threshold was used as a reference point for the pooling of data allowing an alignment of isofrequency contours from different cortices. The use of a single point of reference plus the orientation of the contours does not involve normalization of the length of the dorso-ventral extent of AI. Reale and Imig (1980) gave estimates of the dorso-ventral extent of AI ranging from 4 to 7 mm. However, precise anatomical or physiological criteria for establishing the extent of that dimension are not available (see Middlebrooks and Zook 1983, Schreiner and Mendelson 1990, Sutter and Schreiner 1991a, Schreiner and Cynader 1984, Winer 1984). Therefore, no attempts at extent normalization have been made. A potential consequence of differences in the absolute extent of spatial gradients may be a blurring of the topographies at the dorsal and ventral extremes of the pooled data (see below).

The pooling method did not take into account the actual BF of the units. The question is, then,

could BF sampling biases have strongly affected the observed spatial bandwidth distributions? It has been reported that, with increasing BF, Q-factors of cortical neurons show an overall increase and relative bandwidth values decrease (Phillips and Irvine 1981). Previous studies (Schreiner and Mendelson 1990, Sutter and Schreiner 1991a) had shown only small BF-dependent effects on the dorso-ventral distribution pattern of tuning sharpness, at least for the BF range above 4 kHz which is the same range covered in the current study. In some of the cases included in this study, BFs at locations near the ventral and dorsal end of AI tended to deviate from the projected isofrequency value toward higher frequencies (see Fig. 3C,D). These were also the regions that showed the widest integrative excitatory bandwidth. Since neurons with higher BFs also tend to have narrower bandwidths, a potential BF-influence would tend to diminish the magnitude of the observed bandwidth differences between the dorso-ventral center and the dorsal and ventral margins of AI.

Finally, in interpreting this data, it is important to remember that the recordings from these experiments were limited to depths between 600 and 1000 μm below the cortical surface. Therefore, the presented spatial distribution of single neuron properties may be limited to a portion of AI columns, approximately corresponding to deep layer III and layer IV.

Single Unit vs. Multiple Unit Bandwidth

The multiple unit measurements of sharpness of tuning (excitatory bandwidth 10 and 40 dB above minimum threshold) confirm the spatial pattern in the dorso-ventral dimension of AI as reported for corresponding Q-values (Schreiner and Mendelson 1990, Sutter and Schreiner 1991). All isofrequency contours contain a region of narrow integrated excitatory bandwidths with a gradual transition to more broadly tuned locations toward the ventral and dorsal ends of AI. In other words, the excitatory contributions that are available at different cortical locations along the isofrequency domain appear to systematically vary. What is the source of this gradation in the integrated excitatory bandwidth? Pooled single neuron data dorsal to the minimum in integrated bandwidth 40 dB above threshold showed units with progressively broader bandwidths intermingled with sharply tuned neurons. Local integration of activity from several neurons can account for the observed dorsal bandwidth gradient as reflected in similar slopes of the linear regression for multiple- and single-unit

BW40 (Fig.5). The occurrence of neurons with multi-peaked tuning curves in dorsal AI (Sutter and Schreiner 1991a) contributed to the broadening of the multiple-unit BW40. However, neurons with a single excitatory response area also broadened, occasionally exceeding the total bandwidth of multi-peaked neurons (Fig.5). Broad single-peaked neurons did not necessarily have to reside in close proximity to recorded multi-peaked neurons. It was possible to record any combination of single-peaked broad, single-peaked narrow, and multi-peaked broad neurons in the same penetration. Whether the physiological distinctions of these neurons is paralleled by morphological and/or projectional differences remains to be seen.

Ventral to the minimum in integrated bandwidth, pooled BW40 values of single neurons did not reflect the same trend as seen for the integrated bandwidth. All single neurons in the ventral 3.5 mm of AI remained essentially sharply tuned, that is, below a bandwidth of one octave. By contrast, approximately 25% of the multiple units in that area had bandwidths larger than one octave. Accordingly, no bandwidth gradient was observed for the pooled single neuron data. Some aspects of the pooling method may have contributed to this discrepancy between multiple and single unit measurements. Single units that were located in AII, as defined by multiple unit criteria (Schreiner and Cynader 1984), were not included in the pooled data. A strict definition of the AI/AII border may have biased the single unit distribution toward narrower bandwidths at the ventral end of AI. The distance between the bandwidth minimum and the border of AII could vary over more than 2 mm, even within a single case. Since the length of AI was not normalized for the pooling, a functional gradient between BW40 minimum and AII could be obscured due to the averaging. Indeed, in the most complete single unit case (see Fig. 3), a BW40 gradient is apparent in ventral AI. However, the single unit gradient appears to be somewhat shallower than the multiple-unit gradient. Additionally, even at ventral distances as close as 1 mm from the bandwidth minimum, that is well within AI, the bandwidth discrepancy between single and multiple unit recordings was apparent. There are reasons to believe, then, that the lack of congruence in BW40 for single and multiple units in ventral AI is not solely caused by potential methodological influences but is a reflection of physiological properties that distinguish ventral from dorsal AI (see below).

Discrepancies between single and multiple unit responses were more pronounced for the

measure of BW10. Although the multiple unit BW10 data showed similar gradients along the isofrequency domain as seen for BW40 in this study and for corresponding Q-values in previous studies (Schreiner and Mendelson 1990, Sutter and Schreiner 1991a), pooled BW10 values for single neurons showed no statistically significant bandwidth gradients in either ventral or dorsal AI. The difference between single and multiple units was most strongly expressed in ventral AI with constant average bandwidths across the most ventral 3 mm of AI. In the region dorsal to the multiple unit BW10 minimum, single neuron BW10 values did show a trend similar to the multiple unit data (see Fig. 7C) and paralleling the BW40 results, however, without reaching statistical significance. Contributing to the single/multiple unit discrepancy for BW10 in the dorsal region of AI was the fact that the different peaks in multi-peaked tuning curves show differences in the minimum threshold of each peak (Sutter and Schreiner 1991). Consequently, some of those units are represented by the bandwidth of only one peak and not the total bandwidth across all peaks since minimum threshold of those additional peaks have not been reached 10 dB above the minimum threshold of the most sensitive peak. The lack of a consistent BW10 topography for single neurons reemphasizes the notion that near threshold measurements of sharpness of tuning may not be optimal to assess the sound processing capacities of cortical neurons (Suga and Manabe 1982, Suga and Tsuzuki 1985).

It is concluded that sharply tuned neurons can be found across the entire dorso-ventral extent of AI. The spatial variation in integrated bandwidth in the dorsal region of AI is paralleled by an increase in the scatter of single unit bandwidth and by an increasing occurrence of multi-peaked neurons toward the dorsal end of AI. By contrast, the increase of integrated bandwidth toward the AII border is not necessarily paralleled by an increase in single unit bandwidth. In the approximate dorso-ventral center of AI is a region of sharply tuned single and multiple unit responses.

Influence of BF Scatter on Bandwidth Distribution

The apparent discrepancy between single and multiple unit estimates of the excitatory bandwidth in the ventral portion of AI suggests the influence of other physiological parameters on the bandwidth measures. More specifically, it indicates that near minimum threshold of multiple unit recordings, there are topographical differences in BF scatter and/or scatter in the minimum threshold

of the contributing single neurons. The physiological dorso-ventral center of AI, defined by the multiple unit bandwidth, can only show little BF scatter of single neurons since single and multiple unit responses are equally sharply tuned. An increasing scatter in BF toward the dorsal, and especially ventral borders of AI, could account for the observed increase in multiple unit bandwidth.

As a preliminary test of the hypothesis of a varying degree of BF scatter across AI, a posthoc analysis of single neuron BFs relative to multiple unit BFs was conducted. The BF scatter was determined by one of two methods. If a multiple unit BF was available for the same cortical location as that of a single neuron, the difference between the two BFs was obtained. For single neuron locations that did not coincide with a multiple unit measurement, but were located between at least two multiple unit recording locations, the multiple unit BF at the location of the single neurons was estimated through linear interpolation/triangulation from the actual recording locations and the difference between the estimated multiple unit BF and the actual single neuron BF was obtained. Some single neurons (N=7) had to be excluded from this analysis because expected BF values could not be determined due to lack of appropriately positioned multiple unit recording sites (<500 μ m distance caudal and rostral of the single unit site). The resulting mean BF scatter, expressed in octaves, for 96 single neurons is shown in Fig. 11 for seven 1mm sectors across the dorso-ventral extent of AI (neurons from all 9 cases were included). Near the bandwidth minimum, the obtained mean BF scatter was small and below the mean BW10 values for those locations. More dorsally, and especially more ventrally, the mean BF scatter increased substantially. Although a proper estimate of the distribution of single-unit BF scatter in AI should be done by analyzing several single neurons at each sampled cortical location (e.g. Hui et al. 1989), the currently applied method of comparing multiple unit BFs with single neuron BFs should be a reasonable approximation. The main justifications are that a) multiple unit BFs are likely close to the average of the contributing single neuron BFs, and b) multiple unit BF distributions across AI show a very high degree of cochleotopicity (e.g. Merzenich et al. 1975, Reale and Imig 1980, Schreiner and Mendelson 1990). This preliminary analysis indicates then that the hypothesized spatial change in BF scatter of single neurons is present. Combining the range of BF scatter with the range of single neuron bandwidth for each AI sector results in a good approximation of the overall excitatory bandwidth distribution obtained with multiple unit recording.

How broad multiple unit responses can emerge from narrow single neuron responses can be viewed by considering multiple unit responses as the total integrated excitatory response of the entire recording site (Schreiner and Mendelson 1990). The multiple unit recording could reflect all inputs, inhibitory and excitatory, since this method can potentially record from somas, dendrites and axons of different neurons. With this in mind, the single/multiple unit differences in bandwidth encountered in ventral AI might be due to the inclusion of spikes from proximal inhibitory processes in the vicinity of a post-synaptic neuron into the multiple unit response. Therefore, broad excitatory responses might be due to broad inhibitory inputs of narrowly tuned ventral neurons. If all inputs to a given cortical location, producing either inhibition or excitation, were reflected in multiple unit recordings, dorsally located multi-peaked single neurons should be accompanied by broad single-peaked multiple unit recordings at the same location which, indeed, was often the case (personal observation).

Parceling of AI

Dividing AI into three different regions provided a direct method of addressing questions regarding local differences between single and multiple unit bandwidth measures. The selection of three areas was based on the distribution of the integrated bandwidth alone. The combined results from single and multiple units suggest that, physiologically, AI can be parceled into two regions: a ventral (AIv) and a dorsal (AId) region. The bases of dividing these regions are a) a reversal of the gradient of integrated bandwidth along the dorso-ventral axis of AI, b) regional differences in the distribution of BW40 for single neurons, and c) the observation of neurons with multiple-peaked tuning curves that appear to be limited to the dorsal part of AI.

A significant difference in the spectral integration properties of the granular and supragranular layers of AId and AIv implies that there should be fundamental differences in the spectral processing in the two regions. Functionally, AId may be particularly well-suited for an integrative analysis of broad band stimuli. This is reflected in generally broader excitatory tuning of single neurons as well as by multi-peaked neurons. Additionally, a high responsiveness to broad-band stimuli was observed in AId (Schreiner and Mendelson 1990, Sutter and Schreiner 1991a).

Locations in AIv may be more suited for a differential analysis of the spectral properties of

broad band stimuli since they are characterized by sharply tuned single neurons distributed over varying ranges of BFs. Accordingly, the responsiveness to broad-band stimuli (clicks or white noise) is generally smaller than in AId (Schreiner and Mendelson 1990). However, the distribution of other response parameters, in particular minimum threshold, monotonicity of rate/level functions, and binaurality, have to be taken into account to derive a more complete interpretation of the implications of the described functional topography of AI.

Relation to Previous Studies

The results of this paper may help to resolve discrepancies between various reports of BF topography and sharpness of tuning in AI obtained with single or multiple unit measures. A highly systematic BF topography, the cochleotopic organization, has been reliably found in cat AI when applying the multiple unit recording technique (e.g. Merzenich et al. 1975, Reale and Imig 1980, Schreiner and Mendelson 1990). By contrast, attempts to establish the cochleotopic organization of AI with single unit recordings have indicated limitations on the precision of such an organization on the single neuron level (Erulkar et al. 1956, Bogdanski and Galambos 1960, Evans and Whitfield 1964, Evans et al. 1965, Goldstein et al. 1968, 1970, Abeles and Goldstein 1969). Investigators who reported a lack of BF consistency also report a wide range of tuning sharpness (50% > 0.5 octaves) and a relatively high percentage of multi-peaked neurons. Other studies have claimed that almost all units in AI were sharply tuned (e.g. Phillips and Irvine 1981). The recording of predominantly sharply tuned neurons was possibly due to recording only from the ventral region of AI and/or a reliance on Q-10dB as the measure of sharpness.

Some of the inconsistencies between multiple unit and earlier single unit mapping studies may be accounted for by differences in the extent of the considered cortical area, spatial scatter induced by pooling across animals, and by the state of anesthesia (Merzenich et al. 1975). However, some discrepancies remain such as the range of BF scatter found in single, near-radial penetrations of AI (Evans and Whitfield 1964, Goldstein et al. 1968, Abeles and Goldstein 1970a,b, Phillips and Irvine 1981). The cochleotopicity obtained with the multiple unit technique is derived from the minimum

threshold, that is from the most sensitive neuron or from the average BF of the most sensitive neurons within each cluster. For single neuron studies, an apparent lack of BF topography or even BF consistency within the same penetration (Katsuki et al. 1959a,b, Evans and Whitfield 1964, Goldstein et al. 1968, Goldstein et al. 1970) could be due to recordings from neurons whose thresholds and BFs are different from the most sensitive neuron(s) near the recording location. The preliminary observations in the current study indicate that the precision in the spatial BF distribution of single neurons changes gradually across AI from a strict local alignment in the central 1 to 2 mm of its dorso-ventral extent to a decreasingly strict alignment toward the dorsal and ventral boundaries of AI. This loss of precision in single unit BF organization is present in areas that still show a high degree of cochleotopic organization when tested with multiple unit recordings.

These findings suggest that the integrated multiple unit response is reflecting the mode of the BF distribution at a given location. Single unit studies usually provide only a single sample per location that is subject to the variance in the composition of the local cell assembly. Accordingly, the notion of an isorepresentational frequency domain, i.e. the isofrequency contour, can only be maintained for integrative response measures. The suggestion of a gradually changing variance in the BF distribution of single neurons along the dorso-ventral axis of AI consolidates the picture of the precision in frequency organization as obtained with these different recording methods. Additionally, it provides some of the physiological basis for the observation of gradually changing integrated bandwidths in the cortical dimension orthogonal to the cochleotopic gradient.

Recent studies in primates and birds have indicated that the systematic spatial distribution of integrative excitatory bandwidth, as described earlier (Schreiner and Mendelson 1990, Sutter and Schreiner 1991a) and in this report, might be a general organizational property of the primary auditory telencephalic field. The integrated excitatory bandwidth changes systematically along the isofrequency domain in AI of the owl monkey (Merzenich et al. 1991) in a similar fashion as seen in the cat. In a combined multiple and single unit study of the neostriatal field L in the chick, sharp tuning was found in the approximate center of the isofrequency domain (Heil and Scheich 1991). As in the two mammalian species, an increase in breadth of tuning gradually occurs with recording sites further away from that point.

In conclusion, this study reports a physiological framework of the dorso-ventral extent of AI that is based on the spatial distribution of spectral parameters, namely the excitatory bandwidth (sharpness of tuning) and the best frequency of single as well as local groups of neurons in AI. The presented evidence is compatible with the notion that AI can be divided into at least two functionally separable regions: dorsal AI (AI_d) and ventral AI (AI_v). Functional interpretations of the role of AI from physiological properties of single neurons need to take these topographically based representational principles into account.

ACKNOWLEDGEMENT

We thank Dr. M. M. Merzenich, Dr. G. Recanzone and Marcia Raggio for comments on earlier drafts of the manuscript. The study was partially supported by NIH NS-10414 (to M.M. Merzenich), NIH training grant GM-08155 (to M.L. Sutter), ONR Grant N00014-91-J-1317 (to C.E. Schreiner), Hearing Research Inc., and the Coleman Fund.

Present address of M.L. Sutter: Department of Organismal Biology and Anatomy, 1025 East 57th Street, Chicago, IL 60637.

Address for reprint request: C.E. Schreiner, University of California, San Francisco, Coleman Laboratory, W.M. Keck Center for Integrative Neuroscience, Dept. of Otolaryngology, U494, San Francisco, CA 94143-0732.

REFERENCES

- Abeles, M. and Goldstein, M.H., Jr. Functional architecture in cat primary auditory cortex: columnar organization and organization according to depth. *J. Neurophysiol.* 33: 172-187, 1970a.
- Abeles, M. and Goldstein, M.H., Jr. Responses of single units in the primary auditory cortex of the cat to tones and tone pairs. *Brain Res.* 42:337-352, 1970b.
- Bogdanski, D.V. and Galambos, R. Studies of the auditory system with implanted electrodes. In: *Neural Mechanisms of the Auditory and Vestibular Systems*, edited by G.L. Rasmussen and W.F. Windle. Springfield Ill.: Thomas, 1960, p. 137-151.
- Erulkar, S.D., Rose, J.E., and Davies, P.W. Single unit activity in the auditory cortex of the cat. *Johns Hopkins Hospital Bulletin* 39: 55-86, 1956.
- Evans, E.F. and Whitfield, I.C. Classification of unit responses in the auditory cortex of the unanesthetized and unrestrained cat. *J. Physiol. (London)* 171: 476-493, 1964.
- Evans, E.F., Ross, H.F., and Whitfield, I.C. The spatial distribution of unit characteristic frequency in the primary auditory cortex of the cat. *J. Physiol. (London)* 179: 238-247, 1965.
- Goldstein, M.H., Jr., Abeles, M., Daly, R.L. and McIntosh, J. Functional architecture in cat primary auditory cortex: Tonotopic organization. *J. Neurophysiol.* 33: 188-197, 1970.
- Goldstein, M.H., Jr., Hall, J.L. II, and Butterfield, B.O. Single-unit activity in the primary auditory cortex of unanesthetized cats. *J. Acoust. Soc. Am.* 43: 444-455, 1968.
- Heil, P., and Scheich, H. Functional organization of the avian auditory cortex analogue.
I. Topographic representation of iso-intensity bandwidth. *Brain Res.* 539:110-120, 1991.
- Hind, J.E. Unit activity in the auditory cortex. In: *Neural Mechanisms of the Auditory and Vestibular Systems*, edited by G.L. Rasmussen and W.F. Windle. Springfield Ill.: Thomas, 1960, p. 201-211.
- Hui, G.K., Cassady, J.M. and Weinberger, N.M. Response properties of single neurons within clusters in inferior colliculus and auditory cortex. *Soc. Neurosci. Abstr.* 15: 746, 1989.
- Imig, T.J. & Adrian, H.O. Binaural columns in the primary field (AI) of auditory cortex. *Brain Res.* 138: 241-257, 1977.
- Imig, T.J. and Brugge, J.F. Relationship between binaural interaction columns and commissural

- connections of the primary auditory field (AI) in the cat. *J. Comp. Neurol.* 182: 637-660, 1978.
- Imig, T.J. and Reale, R. Ipsilateral cortico-cortical projections related to binaural columns in cat primary auditory cortex. *J. Comp. Neurol.* 203: 1-14, 1981.
- Katsuki, Y., Watanabe, T. and Maruyama, N. Activity of auditory neurons in upper levels of brain of cat. *J. Neurophysiol.* 22: 343-359, 1959a.
- Katsuki, Y., Watanabe, T. and Suga, N. Interaction of auditory neurons in response to two sound stimuli in cat. *J. Neurophysiol.* 22: 603-623, 1959b.
- Mendelson, J., Schreiner, C.E., Grasse, K., and Sutter, M. Spatial distribution of responses to FM sweeps in cat primary auditory cortex. *Assoc. Res. Otolaryngol. Abstr.* 11: 36, 1988.
- Merzenich, M.M., Knight, P. & Roth, G.L. Representation of the cochlea within the primary auditory cortex in the cat. *J. Neurophysiol.* 38: 231-249, 1975.
- Merzenich, M.M., Schreiner, C.E., Recanzone, G.H., Beitel, R.E., and Sutter, M.L. Topographic organization of cortical field AI in the owl monkey (*aotus trivirgatus*). *Assoc. Res. Otolaryngol. Abstr.* 14, 44, 1991.
- Middlebrooks, J.C. & Zook, J.M. Intrinsic organization of the cat's medial geniculate body identified by projections to binaural response-specific bands in the primary auditory cortex. *J. Neurosci.* 3: 203-224, 1983.
- Middlebrooks, J.C., Dykes, R.W. & Merzenich, M.M. Binaural response-specific bands in primary auditory cortex (AI) of the cat: Topographical organization orthogonal to isofrequency contours. *Brain Res.* 181: 31-48, 1980.
- Phillips, D.P. & Irvine, D.R.F. Responses of single neurons in physiologically defined primary auditory cortex (AI) of the cat: frequency tuning and responses to intensity. *J. Neurophysiol.* 45: 48-58, 1981.
- Reale, R.A. & Imig, T.J. Tonotopic organization in cat auditory cortex. *J. Comp. Neurol.* 192: 265-292, 1980.
- Reale, R.A. and Ketner, R.E. Topography of binaural organization in primary auditory cortex of the cat: effects of changing interaural intensity. *J. Neurophysiol.* 56: 663-682, 1986.
- Rose, J.E. The cellular structure of the auditory region of the cat. *J. Comp. Neurol.* 91: 409-440,

1949.

Schreiner, C.E. and Cynader, M.S. Basic functional organization of second auditory cortical field (AII) of the cat. *J. Neurophysiol.* 51: 1284-1305, 1984.

Schreiner, C.E. and Mendelson, J.R. Functional topography of cat primary auditory cortex: distribution of integrated excitation. *J. Neurophysiol.* 64: 1442-1459, 1990.

Shamma, S.A. and Fleshman, J.W. Spectral orientation columns in the primary auditory cortex. *Assoc. Res. Otol. Abstr.* 13:222, 1990.

Suga, N. and Manabe, T. Neural basis of amplitude-spectrum representation in the auditory cortex of the mustached bat. *J. Neurophysiol.* 47: 225-255, 1982.

Suga, N. and Tsuzuki, K. Inhibition and level-tolerant frequency tuning in the auditory cortex of the mustached bat. *J. Neurophysiol.* 53:1109-1145, 1985.

Sutter, M. and Schreiner, C.E. Physiology and topography of neurons with multi-peaked tuning curves in cat primary auditory cortex. *J. Neurophysiol.* 65, 1207-1226, 1991a.

Sutter, M. and Schreiner, C.E. Spatial distribution of the excitatory bandwidth of single neurons in cat primary auditory cortex. *Assoc. Res. Otol. Abstr.* 13: 21, 1991b.

Winer, J.A. Anatomy of layer IV in cat primary auditory cortex (AI). *J. Comp. Neurol.* 224: 535-567, 1984a.

TABLES:

Table 1: FRA bandwidth measures for single and multiple unit recordings in AI.

	<u>Total</u> §		<u>Dorsal</u> #		<u>Central</u>		<u>Ventral</u>	
	n	Mean±SD	n	Mean±SD	n	Mean±SD	n	Mean±SD
BW40, MU&	146	0.80±0.56	45	0.98±0.59	59	0.57±0.42	42	0.95±0.59
BW40, SU	99	0.50±0.46	29	0.88±0.61	46	0.31±0.24	24	0.40±0.25
BW10, MU	146	0.30±0.24	45	0.35±0.23	59	0.22±0.14	42	0.37±0.32
BW10, SU	103	0.20±0.17	31	0.26±0.21	47	0.19±0.14	25	0.16±0.14

§ Bandwidth expressed in octaves. & SU = Single units; MU = Multiple units. #The central region represents a 2 mm sector of the dorso-ventral extent of AI centered at BW_{min}; the dorsal and ventral regions cover the remainder of AI.

Table 2: Comparison of FRA bandwidth for single and multiple unit measures.

	<u>Dorsal</u> p#	<u>Central</u> p#	<u>Ventral</u> p#
BW40: MU vs. SU	0.51	0.0001	0.0001
BW10: MU vs. SU	0.034	0.099	0.0001

P values from Mann-Whitney U tests.

Table 3: Comparison of FRA bandwidth measures between different sectors of AI.

	<u>Dorsal vs. Central</u> p#	<u>Central vs. Ventral</u> p#	<u>Dorsal vs. Ventral</u> p#
BW40, MU	0.0001**	0.0001**	0.64
BW40, SU	0.0001**	0.13	0.003**
BW10, MU	0.0005*	0.001**	0.96
BW10, SU	0.20	0.50	0.10

P values from Mann-Whitney U tests. ** 99% significance in Scheffe test; * 95% significance in

Scheffe test.

LEGENDS

Figure 1: Frequency response areas (FRAs) for three neurons in AI. A total of 675 tone bursts with different frequency/level combinations were presented. Frequency/level combinations marked with bars elicited action potentials. The height of each bar corresponds to the number of action potentials. The FRAs are plotted for a frequency range of 4 octaves. Bandwidth values were obtained 10 dB (open arrows) and 40 dB (filled arrows) above minimum threshold. Unit A: BF=9.05 kHz, BW10=0.12 octaves (Q-10dB=11.3), BW40=0.26 octaves (Q-40dB=5.66); Unit B: BF=5 kHz, BW10=0.55 oct (2.38), BW40=0.80 oct (1.79); Unit C: BF=9.7 kHz, BW10=1.44 oct (0.70), BW40=2.12 oct (0.49).

Figure 2: Distribution of multiple unit BW10 and BW40 values along the dorsal-ventral axis of for two cortices.

A,B: BW40 values (circles) are connected by dashed lines. Solid lines represent smoothed bandwidth distribution. A spatial weighting algorithm was used for smoothing across 500 μ m sectors: 100% smoothing for points at the same location to no weighting for points 500 μ m apart. Arrows mark the locations with the minimum average BW40 (BW40_{min})

C,D: BW10 values (circles) and smoothed bandwidth distribution. Arrows mark BW10_{min}.

Figure 3: Bandwidth distribution along approximated isofrequency domain of AI (case SUTC16). BW40 (A) and BW10 (B) for single neuron (crosses) and multiple unit (circles) are plotted as a function of cortical distance. BFs of single neurons (C and D) are indicated at the corresponding locations of the BW plots. Zero millimeter of the cortical distance axis corresponds to the location of BW40_{min}.

Figure 4: Demonstration of method used to pool data across animals. The top row (Panels A and C) shows transformation for case SUTC 12. Bandwidths of single neurons 40 dB above minimum

threshold (diamonds) are plotted on same location axis as the multiple unit BW40 map (connected circles). In panel A, the most dorsal location is arbitrarily assigned the value 0 mm. In panel C, $BW_{40\min}$ is assigned a value of 0 mm, and all other locations are referenced as millimeters dorsal (negative) or ventral (positive) from this $BW_{40\min}$. Panels B and D show the same for case SUTC 16 with single neuron BW40's depicted by crosses. $BW_{40\min}$ for the two case is aligned (see panels C and D) and then the single neurons are superimposed within the same coordinate frame (panel E) to yield the pooled result.

Figure 5: Pooled BW40 data . Reference for pooling is the most sharply tuned location 40 dB above threshold of multiple unit responses, $BW_{40\min}$. A) Distribution for all multiple unit recordings (MU). B) Distribution for all single unit recordings (SU). C) Mean value of BW40 over 0.5 mm bins for multiple (light shaded bars) and single (black bars) units. Standard deviations are represented by error bars. The dashed lines in panels A and B correspond to the regression lines derived independently for the areas dorsal and ventral of BW_{\min} .

Figure 6: Distribution of BW40 in three regions of the dorso-ventral dimension of AI ($BF > 4\text{kHz}$). Central region includes area one millimeter to both sides of BW_{\min} for a total of two millimeters. Dorsal region comprises all of AI more than one millimeter dorsal to BW_{\min} , and ventral region more than 1 millimeter ventral to BW_{\min} . A: Histograms of BW40 values for single neurons in AI. B: BW40 for multiple unit recordings. C: Mean values (bars) and standard deviations (error bars) of BW40 values shown in Panels A and B.

Figure 7: Pooled BW10 data. Reference for pooling is the most sharply tuned location 10 dB above minimum threshold of multiple unit responses, $BW_{10\min}$. A) Distribution for all multiple unit recordings. B) Distribution for all single unit recordings. C) Mean value of BW10 over 0.5 mm bins for multiple (light shaded bars) and single (black bars) units. Standard deviations are

represented by error bars. The dashed lines correspond to the regression lines independently derived for the areas dorsal and ventral of $BW_{10\min}$.

Figure 8: Distribution of BW10 in three regions of the dorso-ventral dimension of AI ($BF > 4\text{kHz}$). Central region includes area one millimeter to both sides of BW_{\min} for a total of two millimeters. Dorsal region comprises all of AI more than one millimeter dorsal to BW_{\min} , and ventral region more than 1 millimeter ventral to BW_{\min} . A: Histograms of BW10 values for single neurons in AI. B: BW10 for multiple unit recordings. C: Mean values (bars) and standard deviations (error bars) of BW10 values shown in panels A and B.

Figure 9: Estimated scatter of BF as a function of cortical location. Expected BF for single unit locations was interpolated by 3 point triangulation from multiple unit maps or by multiple unit BF at same recording location. This was possible for 96 out of 103 single units. $BF\ scatter = \text{single neuron } BF - \text{expected } BF$. Values were then averaged over one mm of the dorso-ventral extent of AI to derive a mean BF scatter value. The number of neurons in each of the seven bins (from dorsal to ventral) were 9, 13, 12, 28, 20, 8, and 6, respectively. The standard deviations of the BF scatter (in octaves) for the seven sectors were: 0.27, 0.35, 0.34, 0.09, 0.13, 0.88, and 0.60.

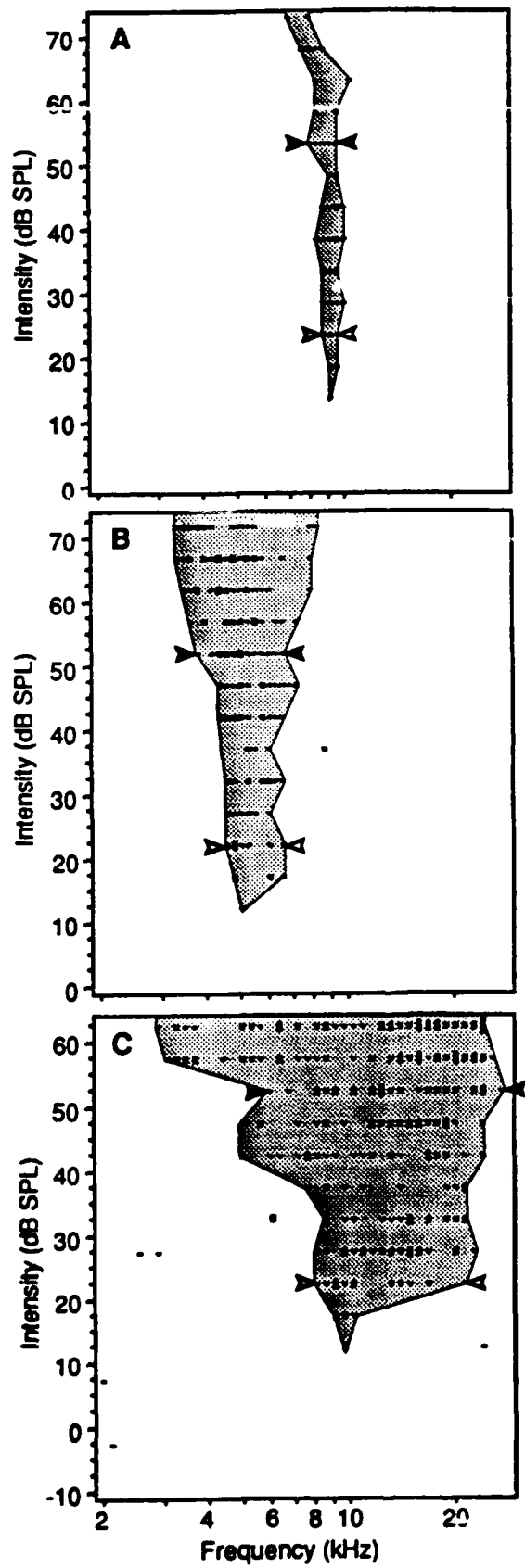
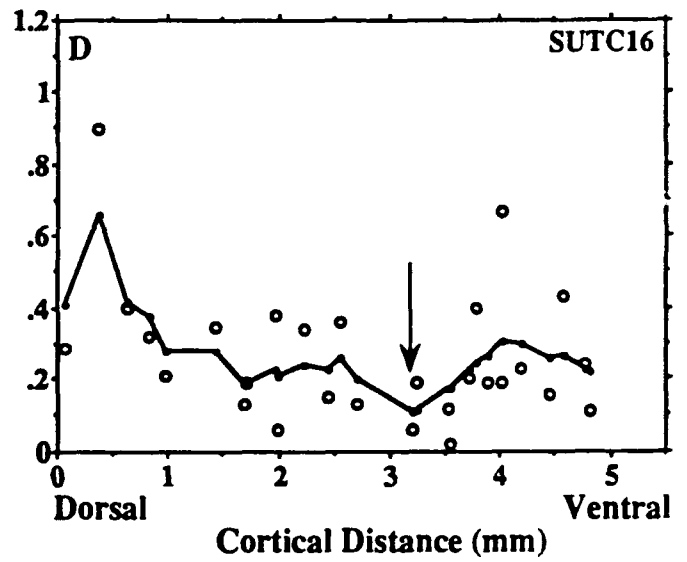
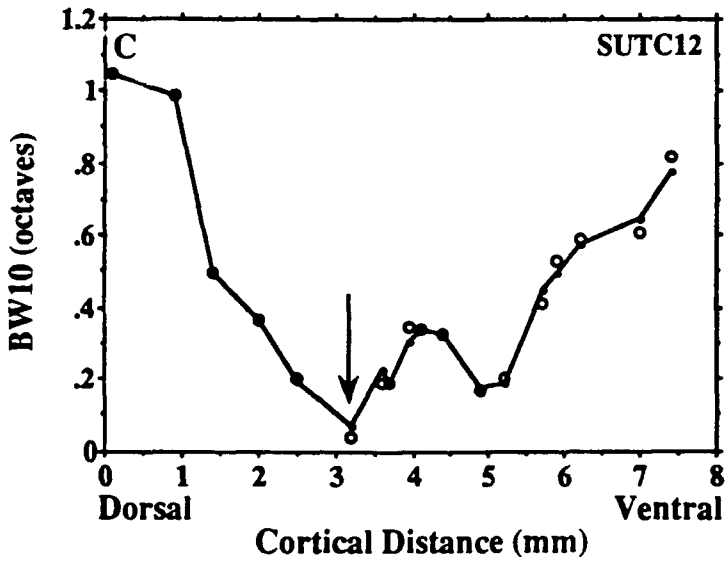
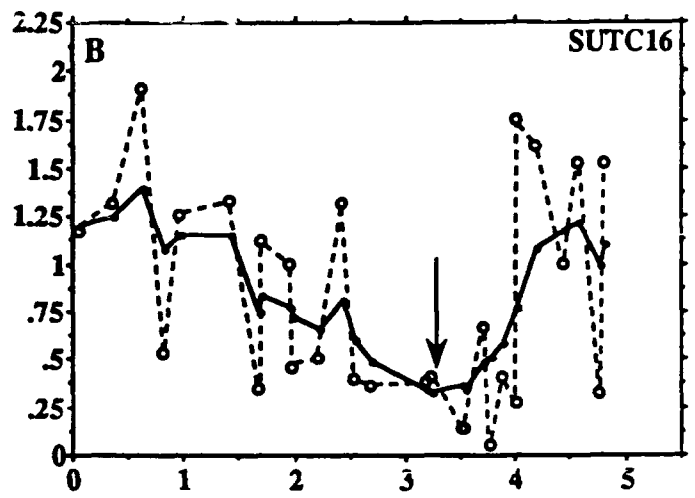
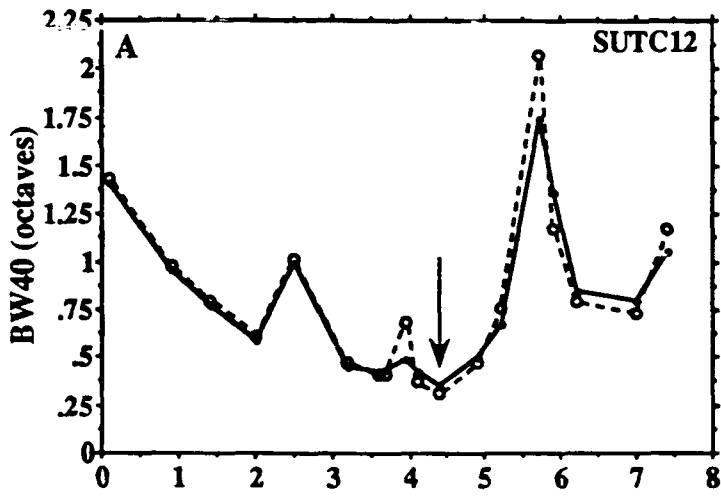
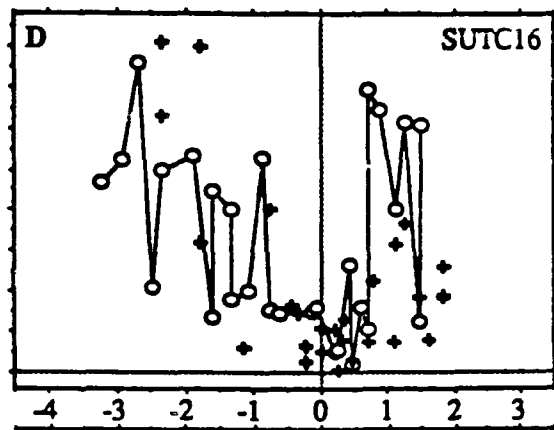
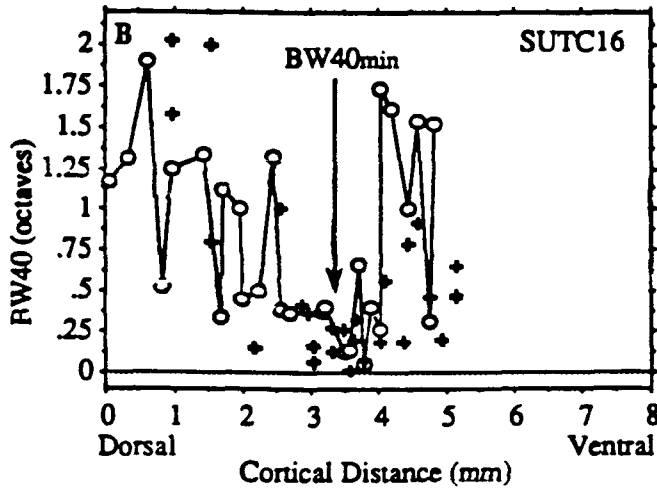
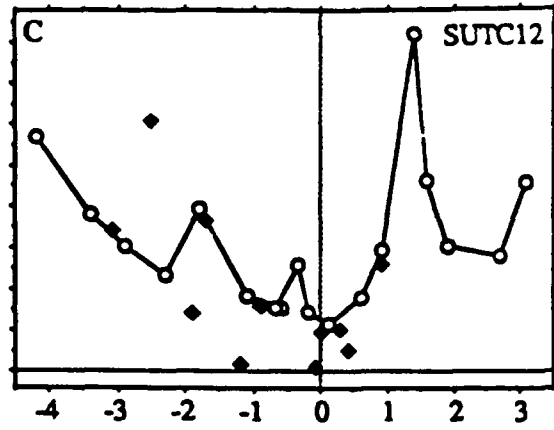
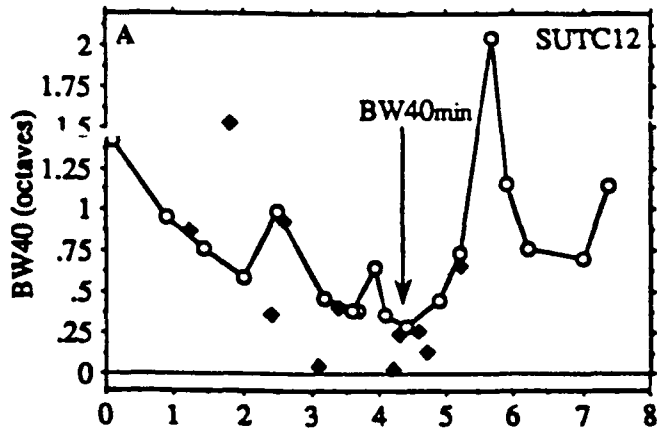
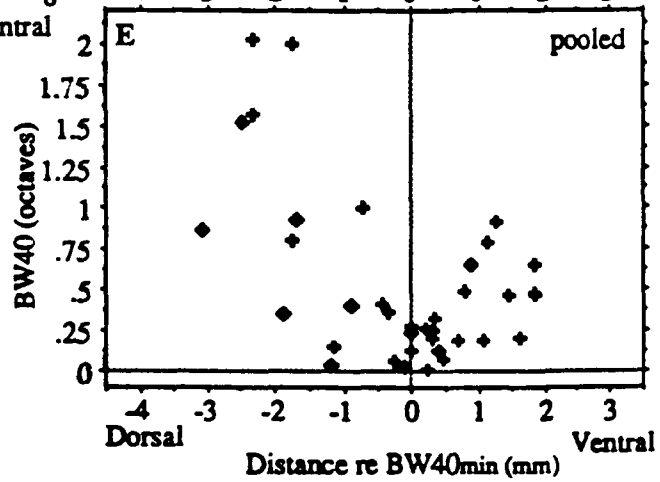


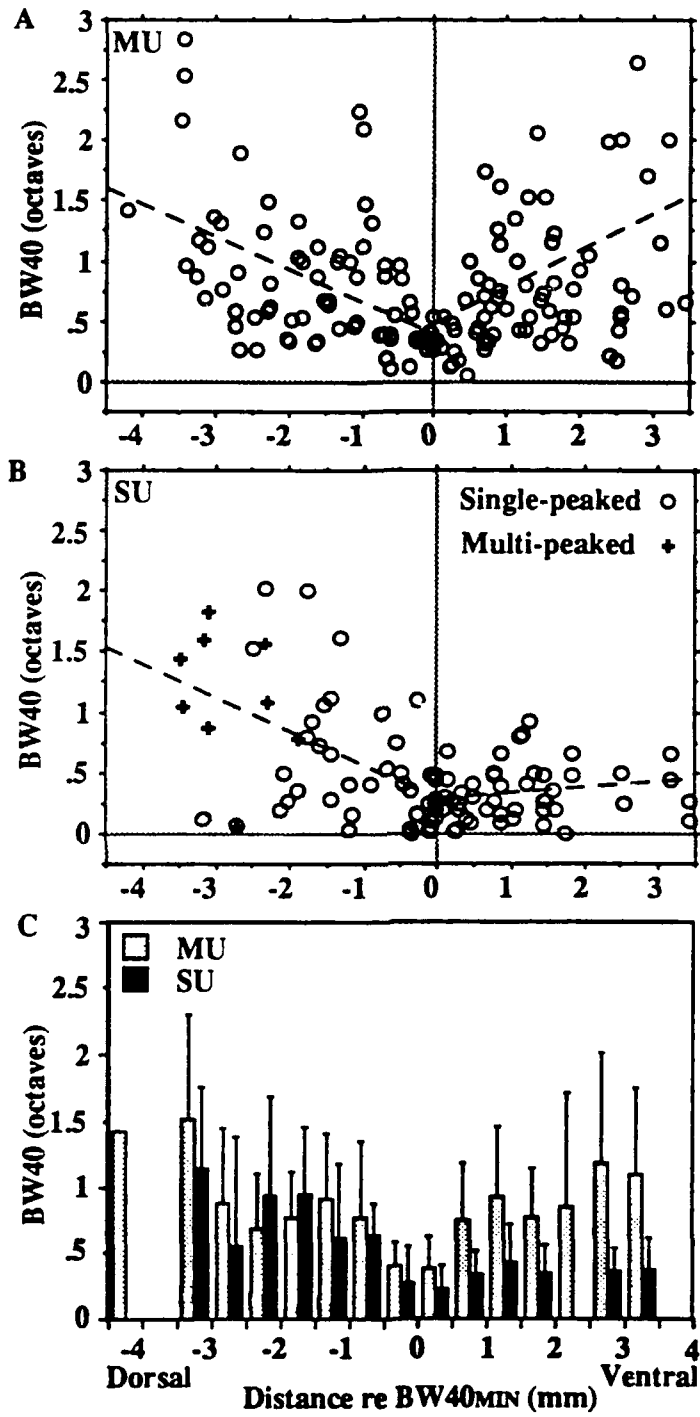
Fig 1





- ◆ Single Units SUTC12
- ◆ Single Units SUTC16
- Multiple Units





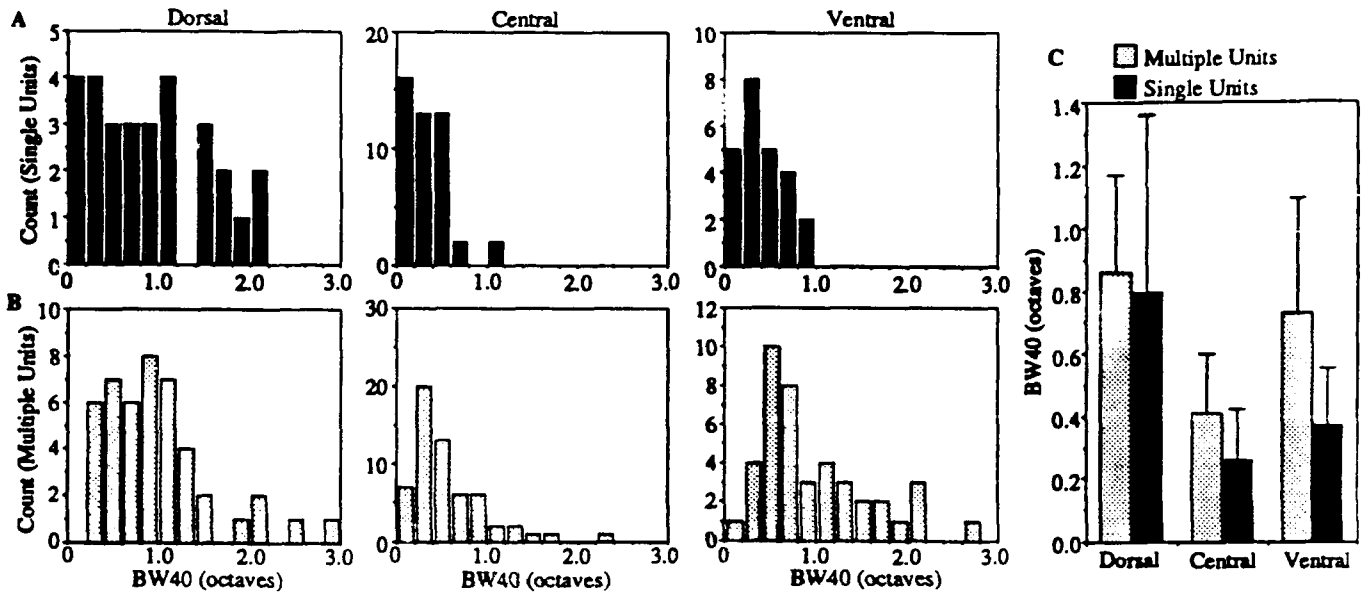
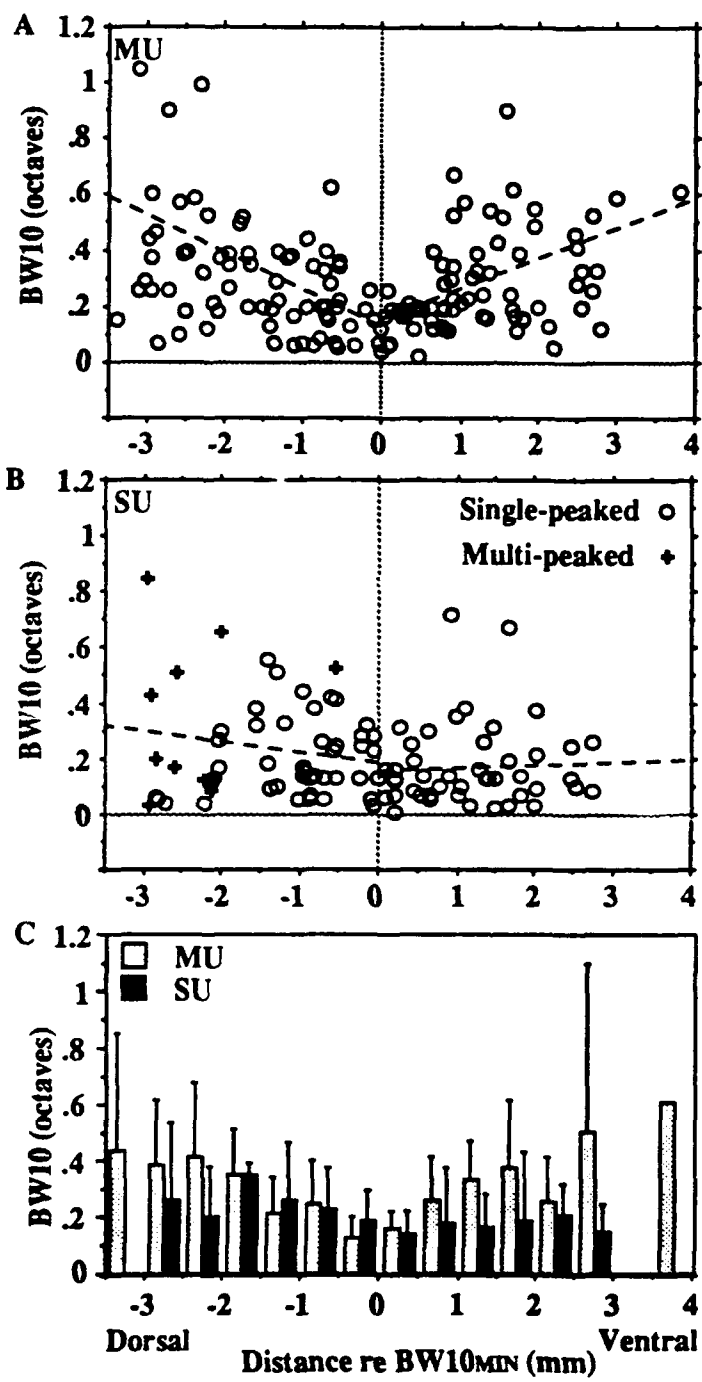
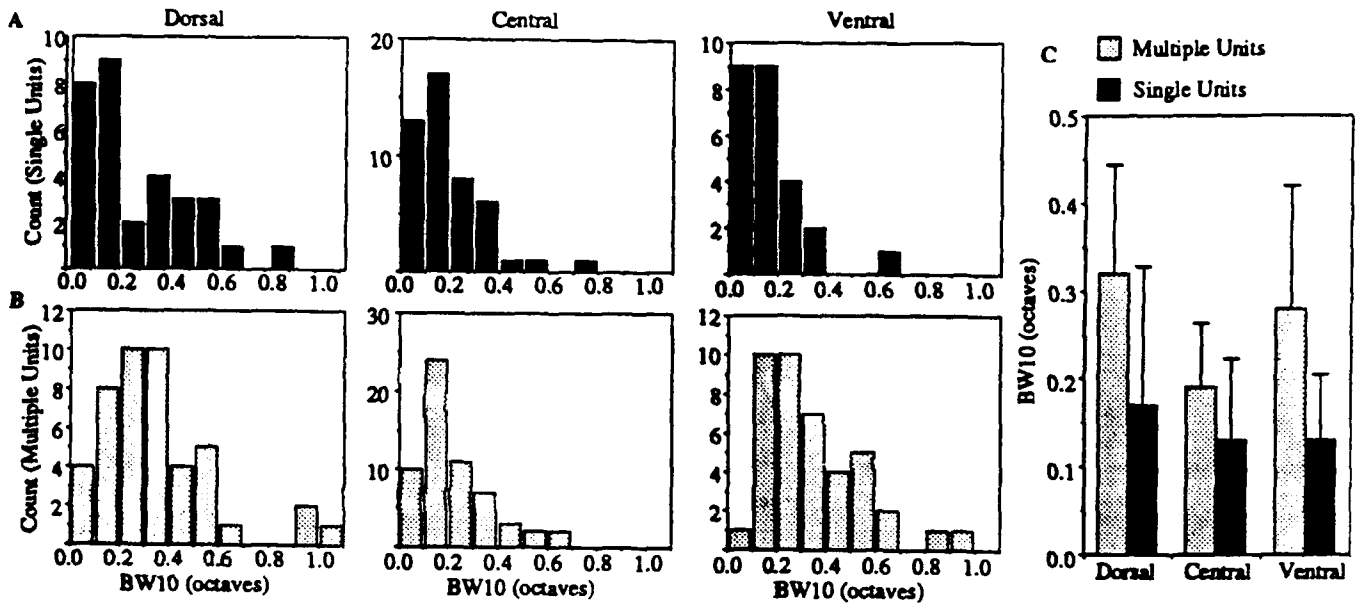
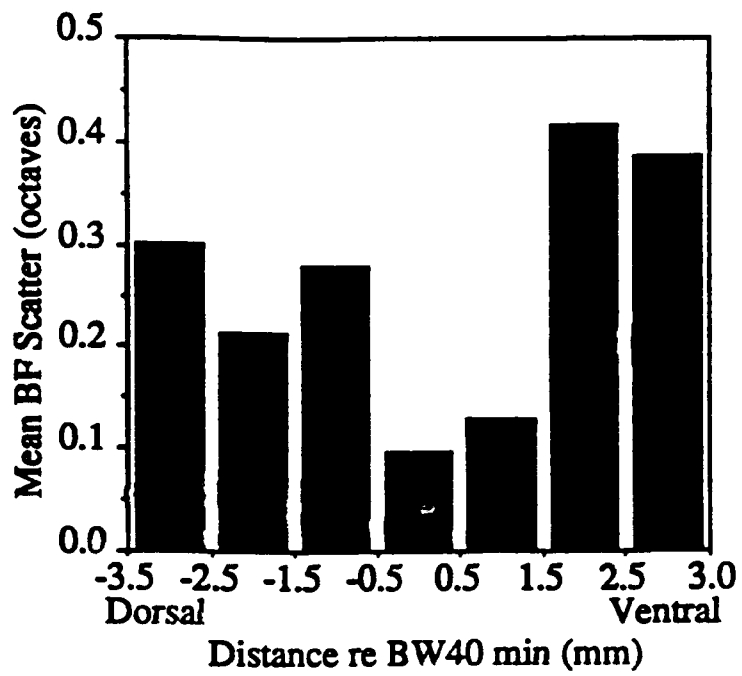


Fig 5





7.8 29



Appendix B:

Copy of Letter from Dr. Kamil Grajski

May 30, 1991

Dr. Harold Hawkins
Dr. Teresa McMullen
Office of Naval Research, Neural Sciences Division
800 North Quincy Street, Room 823
Arlington, VA 22217-5000

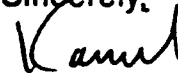
Dear Harold:

This letter is to officially inform you of a change in my employment status which, happily, positively affects my ability to contribute to the Bioacoustic Signal Classification in Cat Auditory Cortex Study run by Chris Schreiner.

I have moved from what was Ford Aerospace (now Loral Aerospace) to Apple Computer in Cupertino, California. My position is Senior Scientist in the Speech and Language Technologies department within the Advanced Technology Group. Some of my colleagues are world-renowned researchers in the field of speech recognition research, e.g., Kai-Fu Lee, Bruce Lowerre, George White. In addition, I interact with Dick Lyon and his associate Malcolm Slaney specifically on the subject of using their peripheral models as a front-end to the SPHINX speech recognition system. My own work is currently aimed at achieving better acoustic modeling for multiple-codebook HMM-based recognizers. We are also looking at HMM-Neural Network hybrids.

The overall effect is positive for several reasons. First, direct access to Dick Lyon has resulted in his willingness to work with us during the phase of the project where we discuss peripheral modeling. He has already contributed a technical report and Macintosh disks with source code, etc. His interaction will nicely complement Ted Lewis' contributions. Second, since I am in a Speech and Language group, Apple understands the importance of such a project; they appear to be supportive and flexible concerning my participation. Third, facilities here are superb! Apple owns its own CRAY, and the latest Mac and Sun computers. Last, through a steady stream of visitors, interns and hearing research seminars, there is access to an active, interested and well-informed community of scientists. The work will not be done in isolation.

Sincerely,



Kamil A. Grajski

cc:C. Schreiner

New phone # 408-974-1313

91 6 18 013